Telomere Binding of Checkpoint Sensor and DNA Repair Proteins Contributes to Maintenance of Functional Fission Yeast Telomeres

Toru M. Nakamura,[1,2] Bettina A. Moser[1] and Paul Russell

Departments of Molecular Biology and Cell Biology, The Scripps Research Institute, La Jolla, California 92037

Manuscript received March 6, 2002
Accepted for publication May 22, 2002

ABSTRACT

Telomeres, the ends of linear chromosomes, are DNA double-strand ends that do not trigger a cell cycle arrest and yet require checkpoint and DNA repair proteins for maintenance. Genetic and biochemical studies in the fission yeast *Schizosaccharomyces pombe* were undertaken to understand how checkpoint and DNA repair proteins contribute to telomere maintenance. On the basis of telomere lengths of mutant combinations of various checkpoint-related proteins (Rad1, Rad3, Rad9, Rad17, Rad26, Hus1, Crb2, Chk1, Cds1), Tel1, a telomere-binding protein (Taz1), and DNA repair proteins (Ku70, Rad32), we conclude that Rad3/Rad26 and Tel1/Rad32 represent two pathways required to maintain telomeres and prevent chromosome circularization. Rad1/Rad9/Hus1/Rad17 and Ku70 are two additional epistasis groups, which act in the Rad3/Rad26 pathway. However, Rad3/Rad26 must have additional target(s), as cells lacking Tel1/Rad32, Rad1/Rad9/Hus1/Rad17, and Ku70 groups did not circularize chromosomes. Cells lacking Rad3/Rad26 and Tel1/Rad32 senesced faster than a telomerase *trt1*Δ mutant, suggesting that these pathways may contribute to telomere protection. Deletion of *taz1* did not suppress chromosome circularization in cells lacking Rad3/Rad26 and Tel1/Rad32, also suggesting that two pathways protect telomeres. Chromatin immunoprecipitation analyses found that Rad3, Rad1, Rad9, Hus1, Rad17, Rad32, and Ku70 associate with telomeres. Thus, checkpoint sensor and DNA repair proteins contribute to telomere maintenance and protection through their association with telomeres.

CHECKPOINT and DNA repair pathways are crucial to the progression of the normal cell cycle. Without them, cells cannot maintain a stable genome, and genetic instability can lead to cell death, cancer, and other genetic disorders (Khanna and Jackson 2001). The DNA replication checkpoint prevents mitosis until DNA is replicated completely. Similarly, the DNA damage checkpoint inhibits mitosis in response to damaged DNA. Checkpoint controls are highly conserved. Homologs to many checkpoint proteins that were originally identified in yeasts have now been found in multicellular eukaryotes, including humans. Checkpoint proteins form signaling cascades activated by a DNA replication block or DNA damage and subsequently generate the negative constraints on cell cycle progression (Rhind and Russell 1998). One form of DNA damage recognized by checkpoint proteins is the double-strand break (DSB). DSBs may be created as a part of cell cycle events, such as DNA replication and meiotic recombination, or by exposure to genotoxic chemicals or ionizing radiation. DSBs are repaired by either homologous recombination or nonhomologous end joining (NHEJ).

Telomeres, the natural ends of linear chromosomes, are maintained by the specialized reverse transcriptase called telomerase. Many proteins bind telomeric DNA and protect it from degradation and recombination. Telomeres pose special challenges to the DNA repair machinery and checkpoint proteins because these DNA ends must be maintained, unlike other internal DSBs, which must be rejoined (Blackburn 2001). Therefore, one might expect the DNA repair and checkpoint machinery to be excluded from telomeres. Surprisingly, studies from the budding yeast *Saccharomyces cerevisiae* and mammalian cells suggest that proteins required for NHEJ, such as the Ku70-Ku80 heterodimer and the Mre11-Rad50-Xrs2 complex (Mre11-Rad50-Nbs1 in mammalian cells), are present at telomeres and are needed for normal telomere functions (Nugent *et al.* 1998; Ritchie and Petes 2000; Zhu *et al.* 2000; Tsukamoto *et al.* 2001). Likewise, studies in *S. cerevisiae* and in the fission yeast *Schizosaccharomyces pombe* suggest that rather than being denied access to telomeres, the checkpoint sensor proteins, such as budding yeast Mec1 and fission yeast Rad3, seem to recognize telomeres (Dahlén *et al.* 1998; Naito *et al.* 1998; Matsuura *et al.* 1999; Ritchie *et al.* 1999; Longhese *et al.* 2000). Yet, these checkpoint sensors are somehow prevented from activating checkpoints when they interact with the DNA ends at telomeres.

Using the fission yeast *S. pombe* as a model system, we wished to understand how this apparent alteration in the checkpoint signaling pathways at telomeres is

[1] These authors contributed equally to this work.

[2] *Corresponding author:* Department of Molecular Biology, MB3, The Scripps Research Institute, 10550 N. Torrey Pines Rd., La Jolla, CA 92037. E-mail: nakamut@scripps.edu

achieved to allow the DNA structure checkpoint proteins to recognize telomeres as the unique DNA ends that should not be repaired. Advantages of the fission yeast system include well-characterized DNA damage responses with high structural and functional conservation to the mammalian system; amenability to genetic, biochemical, and cytological studies; and a small number of telomeres per cell. In addition, the ability of fission yeast to bypass the need for a functional telomere maintenance mechanism by circularizing all chromosomes (Naito *et al.* 1998; Nakamura *et al.* 1998) provides flexibility, not available in any other organisms, in manipulating telomere-related genes without being hindered by cell lethality.

The DNA structure checkpoint responses in *S. pombe* require a group of six "checkpoint Rad proteins" (Rad1, Rad3, Rad9, Rad17, Rad26, and Hus1), which are thought to function as sensors of DNA replication arrest and DNA damage (Caspari and Carr 1999). Rad1, Rad9, and Hus1 proteins have weak sequence similarity to proliferating cell nuclear antigen (PCNA) and form a ring-shaped complex (Caspari *et al.* 2000; Kaur *et al.* 2001; Griffith *et al.* 2002). Rad17 protein shows sequence similarity to replication factor C (RFC) proteins (Griffiths *et al.* 1995) and associates with other RFC subunits (Kai *et al.* 2001). Since the RFC complex recruits PCNA onto DNA, it has been proposed that the Rad17 complex loads the Rad1-Rad9-Hus1 complex onto sites of DNA damage. Rad3 is related to human ATM and Rad3-related (ATR) and ataxia telangiectasia-mutated (ATM) protein kinases, the latter of which is mutated in patients with the cancer-prone genetic disorder ataxia-telangiectasia. Rad3 is stably associated with its regulatory subunit Rad26 (Edwards *et al.* 1999; Wolkow and Enoch 2002). Two additional proteins, Crb2 and Cut5, are also implicated in the DNA damage checkpoint (Saka *et al.* 1997), but they appear to function downstream of the checkpoint Rad proteins. Mutations in *rad1*, *rad3*, *rad17*, and *rad26* cause telomere shortening (Dahlén *et al.* 1998). Therefore, checkpoint sensor proteins appear to have a positive role in maintaining telomere length.

In addition to Rad3, *S. pombe* cells have another protein kinase related to ATR and ATM called Tel1, and the phenotype of *rad3*Δ *tel1*Δ illustrates the importance of ATR and ATM family proteins in telomere maintenance. The double-mutant cells have dramatically shortened telomeres, and the cells often lose their telomeres completely and circularize all chromosomes (Naito *et al.* 1998), much like survivors of a telomerase deletion mutant strain (*trt1*Δ; Nakamura *et al.* 1998). Rad3 and Tel1 might be needed simply for a delay in the cell cycle to allow telomerase to complete telomeric DNA synthesis, with chromosomal fusions being the secondary consequence of the ensuing loss of telomeric repeats. Alternatively, Rad3, Tel1, and other checkpoint proteins might act directly at telomeres to allow cells to distinguish telomeres from other types of DNA ends or to recruit telomerase to telomeres. As the ATR and ATM family kinases also show sequence similarity to the catalytic subunit of DNA-protein kinase (DNA-PK), which binds and is activated by broken DNA ends, Rad3 and Tel1 might bind directly to telomeric DNA. Binding of DNA-PK to telomeric DNA has been reported in mammalian cells (d'Adda di Fagagna *et al.* 2001).

Studies of telomere length in cells carrying mutations in the DNA damage checkpoint downstream signal transducer proteins support a more direct role for the checkpoint Rad proteins in telomere length maintenance (Dahlén *et al.* 1998; Matsuura *et al.* 1999). In *S. pombe*, the Chk1 and Cds1 protein kinases work downstream of the checkpoint Rad proteins to transmit the signals created in response to DNA damage and replication blocks to the cyclin-dependent kinase Cdc2 regulators Cdc25 and Mik1 (Rhind and Russell 1998). Despite the involvement of the checkpoint Rad proteins in telomere length maintenance, mutations of Chk1, Cds1, and another Cdc2 regulator Wee1 or overexpression of Cdc25 have no effect on telomere length; nor do mutations in Cdc2 affect telomere length (Dahlén *et al.* 1998). Therefore, telomere length maintenance in *S. pombe* appears to be independent of cell cycle arrest that involves the regulation of Cdc2. Conceivably, functional telomeres might inhibit interactions between checkpoint Rad proteins and checkpoint downstream signaling transducers. The checkpoint Rad proteins might even have unidentified alternate downstream signal transducers that are used to ensure telomere replication.

To define the roles that checkpoint and DNA repair proteins play in telomere maintenance, we undertook epistasis analysis of various checkpoint and DNA repair mutants on the basis of steady-state telomere length in a series of multiple mutant combinations. From these studies, we conclude that Rad3/Rad26 and Tel1/Rad32 represent two independent functional pathways required for the maintenance of stable telomeres (Rad32 is an ortholog of the *S. cerevisiae* and mammalian Mre11 proteins). We also compared senescence rates upon telomerase *trt1* deletion in various checkpoint mutant backgrounds and conclude that Rad3/Rad26 and Tel1/Rad32 pathways must also be important for functions other than the recruitment of telomerase to telomeres. In addition, we show that damage-induced phosphorylation of Rad32 is independent of both Rad3 and Tel1 kinases, and we thus implicate other unidentified kinase(s) in phosphorylation of Rad32. We also demonstrate specific association of checkpoint sensor and DNA repair proteins to telomeres by chromatin immunoprecipitation (ChIP) analyses. Through these studies we conclude that checkpoint sensor and DNA repair pro-

teins contribute to maintenance and protection of telomeres through their binding to telomeres.

MATERIALS AND METHODS

Yeast strains and general methods: The fission yeast strains used in this study were constructed by standard techniques (Alfa *et al.* 1993). Most strains used in this study are *leu1-32 ura4-D18 his3-D1 ade6-M210* or *ade6-M216*, and detailed genotypes are listed in the supplementary Table S1 at http://www.genetics.org/supplemental. Sequences of PCR oligonucleotide primers used for strain construction are listed in the supplementary Table S2 at http://www.genetics.org/supplemental.

Mutations were previously described for *rad1*Δ (*rad1::ura4*$^+$; Sunnerhagen *et al.* 1990), *rad9*Δ (*rad9::ura4*$^+$; Murray *et al.* 1991), *hus1*Δ (*hus1::LEU2*; Kostrub *et al.* 1997), *rad17*Δ (*rad17::ura4*$^+$; Griffiths *et al.* 1995), *rad3*Δ (*rad3::ura4*$^+$; Bentley *et al.* 1996), *rad26*Δ (*rad26::ura4*$^+$; al-Khodairy *et al.* 1994), *crb2*Δ (*crb2::ura4*$^+$; Saka *et al.* 1997), *chk1*Δ (*chk1::ura4*$^+$; al-Khodairy *et al.* 1994), *cds1*Δ (*cds1::ura4*$^+$; Boddy *et al.* 1998), and *trt1*Δ (*trt1-D2::his3*$^+$; Nakamura *et al.* 1997). Strains carrying *nmt-HA-rad3* (Moser *et al.* 2000) and *taz1-HA* (Kanoh and Ishikawa 2001) were also described previously.

For *taz1*Δ, a PCR-based method (Bähler *et al.* 1998) was used to create *taz1-D3::LEU2* (taz1-LEUT and taz1-LEUB primers) and *taz1-D4::kanMX4* (taz1-MX4T and taz1-MX4B primers). In addition, a previously described *taz1::ura4*$^+$ mutation (Cooper *et al.* 1997) was PCR amplified from genomic DNA (tazKO-LU and tazKO-RB primers). These PCR products were then used for *taz1* gene deletion in various checkpoint and DNA repair mutant strain backgrounds.

A PCR-based method (Bähler *et al.* 1998) was used to create *rad32*Δ (*rad32-D1::kanMX4*), using rad32-KO1 and rad32-KO2 primers; *pku70*Δ (*pku70-D1::kanMX4*), using pku70-KO1 and pku70-KO2 primers; and *rad3*Δ (*rad3-D2::LEU2*), using rad3-LEUT and rad3-LEUB primers.

For *tel1*Δ (*tel1-D1::kanMX4*), the carboxy-terminal untranslated region was amplified by PCR (tel1-T1 and tel1-B2 primers) and then cloned into pBluescript II SK(+) (Stratagene, La Jolla, CA) as a *Hin*dIII-*Xho*I fragment. The amino-terminal untranslated region was subsequently amplified (tel1-T3 and tel1-B4 primers) and cloned into the same plasmid as the *Sac*I-*Xba*I fragment. This plasmid was then digested with *Bam*HI and *Eco*RI to clone the *Bam*HI-*Eco*RI kanMX4 fragment from the pFA6a-kanMX4 plasmid (Wach *et al.* 1994), creating pBS-tel1::kanMX4 plasmid. The *Sac*II-*Sna*BI *tel1::kanMX4* fragment from pBS-tel1::kanMX4 was then used for *tel1* deletion. Another *tel1*Δ (*te11-D2::LEU2*) was created by a PCR-based method (Bähler *et al.* 1998), using tel1-LEUT and tel1-LEUB primers.

A PCR-based method (Bähler *et al.* 1998) was used to create carboxy-terminally tagged *rad32-TAP* and *rad32-myc* (rad32-tagT and rad32-tagB primers), *pku70-myc* and *pku70-HA* (BAM102 and BAM103 primers), *rad9-myc* (BAM84 and BAM85 primers), and *hus1-myc* (BAM88 and BAM89 primers). Another PCR technique (Krawchuk and Wahls 1999) was used to create carboxy-terminally tagged *rad1-myc* (BAM36–BAM39 primers) and *rad17-myc* (BAM31–BAM34 primers).

HA-rad3 cells express the amino-terminally 3HA-tagged Rad3 fusion protein from the endogenous *rad3*$^+$ promoter. It was created by transforming a strain with an integrated *ura4*$^+$ marker 5′ adjacent to the *rad3*$^+$ gene with the plasmid carrying the *3HA-rad3* fusion construct and then selecting for 5-fluoroorotic acid (5-FOA)-resistant cells (Grimm *et al.* 1988).

Pulsed-field gel electrophoresis: For pulsed-field gel electrophoresis (PFGE), cells were suspended and lysed in agarose plugs as follows: Cells were washed twice in SP1 [50 mm citrate-phosphate (pH 5.6), 40 mm EDTA, 1.2 m sorbitol] and then incubated for 2–3 hr at 37° in SP1 with 0.6 mg/ml Zymolyase-100T (ICN Biomedicals). The cells were pelleted and resuspended at 6–7 × 10^8 cells per ml in TSE [10 mm Tris-HCl (pH 7.5), 0.9 m sorbitol, 45 mm EDTA]. The cell suspension was warmed to 42°, and 1–1.5 volume of 1% low-melting agarose (Bio-Rad, Richmond, CA) in TSE was added. Aliquots were dispensed into plug molds and allowed to solidify. The gelled plugs were incubated at 55°, first for ~90 min in 0.25 m EDTA, 50 mm Tris-HCl (pH 7.5), and 1% SDS and then for 48 hr in 1% lauryl sarcosine, 0.5 m EDTA (pH 9.5), and 1 mg/ml proteinase K. Plugs were washed three times in Tris-EDTA and stored at 4° in Tris-EDTA. For *Not*I-digested PFGE, plugs were preequilibrated 2–3 hr at 37° in NEB3 buffer [10 mm NaCl, 5 mm Tris-HCl, 1 mm $MgCl_2$, 0.1 mm dithiothreitol (pH 7.9 at 25°)] plus 100 μg/ml BSA and then digested with *Not*I restriction endonuclease at 37° overnight. Probes specific for telomeric *Not*I fragments (C, I, L, and M) were created as previously described (Nakamura *et al.* 1998).

Liquid culture growth curve: Heterozygous diploid strains were sporulated and the resulting tetrads were dissected and germinated on yeast extract medium-supplemented (YES) plates (Alfa *et al.* 1993); genotypes of the resulting cells were then distinguished by growing them on selective minimal plates. Colonies derived from each spore were grown at 32° for 3 days and then picked and diluted to 5 × 10^4 cells/ml in 20 ml YES. These cultures were grown for 24 hr at 32°, at which point the cell density was determined by counting in a hemacytometer, and the cells were diluted to a cell density of 5 × 10^4 cells/ml in 20 ml fresh YES liquid medium and incubated at 32°. These procedures were repeated every 24 hr for 18 days.

Immunopurification and Western blot analysis: Whole-cell extracts from *rad32-TAP*-tagged (Rigaut *et al.* 1999) strains were purified with IgG Sepharose (Pharmacia, Piscataway, NJ). Purified material was analyzed by Western blot analysis using peroxidase anti-peroxidase (PAP) antibody (P 2026; Sigma, St. Louis). λ protein phosphatase (New England Biolabs, Beverly, MA) was used to perform phosphatase treatment.

ChIP assays: ChIP assays were performed as described (Strahl-Bolsinger *et al.* 1997) with minor modifications. Cells were lysed in lysis buffer (50 mm Hepes-KOH pH 7.5, 140 mm NaCl, 1 mm EDTA, 1% Triton X-100, 0.1% sodium deoxycholate, 5 μg/μl aprotinin, 5 μg/μl leupeptin, 5 μg/μl pepstatin, 1 mm phenylmethylsulfonyl fluoride). The crude cell lysate was sonicated to yield 0.5–1 kb DNA fragments and clarified by centrifugation for 10 min at 16,000 × *g*. Prior to immunoprecipitation, 1/10 volume of the cell lysate was saved for an input control. Immunoprecipitations were performed with either monoclonal anti-myc antibody (9E10; Babco) or monoclonal anti-HA antibody (16B12; Babco). Immunoprecipitates were washed three times each with 1 ml lysis buffer and 1 ml lysis buffer/500 mm NaCl and two times each with 1 ml wash buffer (10 mm Tris-HCl pH 8, 0.25 m LiCl, 0.5% NP-40, 0.5% sodium deoxycholate, 1 mm EDTA) and 1 ml TE buffer (10 mm Tris-HCl, 1 mm EDTA pH 8). The samples were then processed as described (Orlando and Paro 1993). PCR reactions used the following primers to amplify the telomeric DNA (BAM136, 5′ GTG TGG AAT TGA GTA TGG TGA A 3′; BAM137, 5′ CGG CTG ACG GGT GGG GCC CAA TA 3′) or the *ade6*$^+$ DNA (BAM138, 5′ AGG TAT AAC GAC AAC AAA CGT TGC 3′; BAM139, 5′ CAA GGC ATC AGT GTT AAT ATG CTC 3′). To assure a quantitative analysis between individual samples, we first established that we assayed in the

linear range of the PCR. PCR reactions were analyzed on 2% agarose gels in 1× TAE buffer.

RESULTS

Checkpoint sensor mutants all have shorter telomeres: Previous studies in *S. pombe* reported that *rad1*, *rad17*, *rad3*, and *rad26* mutant cells have shorter telomeres, while *rad9* and *hus1* mutant cells have normal telomere length (Dahlén *et al.* 1998; Naito *et al.* 1998; Matsuura *et al.* 1999). Rad1, Rad9, and Hus1 share a PCNA-like motif (Cai *et al.* 2000; Venclovas and Thelen 2000), form a heterotrimeric complex, and appear to function in a single pathway with regard to checkpoint responses (al-Khodairy *et al.* 1994; Kostrub *et al.* 1997; Caspari *et al.* 2000; Kaur *et al.* 2001). Therefore, it was surprising to find that *rad1* mutant cells have shortened telomeres while *rad9* and *hus1* mutant cells have normal telomere lengths. However, many of the checkpoint mutant cells tested in previous studies were point mutations, and thus it was possible that some checkpoint proteins were erroneously found not to play a role in telomere maintenance. Therefore, we decided to retest telomere length in deletion mutants of checkpoint sensor proteins (Rad1, Rad9, Hus1, Rad17, Rad3, and Rad26) and their downstream effector proteins (Crb2, Chk1, and Cds1).

In contrast to previous reports, we found that *rad1*Δ, *rad9*Δ, and *hus1*Δ strains all had shorter telomeres (Figure 1A, lanes 2–4; Figure 2A). In addition, the *rad17*Δ mutant strain had shorter telomere length and the extent of shortening was similar to that of *rad1*Δ, *rad9*Δ, and *hus1*Δ strains (Figures 1A and 2A). *rad3*Δ and *rad26*Δ cells had the shortest telomere lengths among the six checkpoint sensor mutants (Figure 1A, lanes 7 and 8; Figure 2A). Mutations in other checkpoint-related proteins (*crb2*Δ, *chk1*Δ, *cds1*Δ, and *chk1*Δ *cds1*Δ) that are thought to function downstream of the six checkpoint sensor proteins had little or no effect on telomere length (Figure 1A, lanes 9–13; Figure 2A).

We further analyzed telomere length in various double-mutant combinations among checkpoint sensor proteins (Figure 1B) and found that *rad1*Δ *hus1*Δ, *rad9*Δ *hus1*Δ, and *rad17*Δ *hus1*Δ mutant combinations have the same telomere length as the single mutants (Figure 1B, lanes 2–8; Figure 2B). These results suggest that *rad1*Δ, *rad9*Δ, *hus1*Δ, and *rad17*Δ function in a single pathway for telomere maintenance, consistent with their function in the checkpoint response (al-Khodairy and Carr 1992). Rad3 and Rad26 appear to function in the same pathway, as the *rad3*Δ *rad26*Δ double mutant had the same telomere length as the single mutants (Figure 1B, lanes 9–11; Figure 2B; Matsuura *et al.* 1999). Mutations in *rad3* and *rad26* are epistatic to *rad1*, *rad9*, *hus1*, and *rad17*, since *rad3*Δ *rad1*Δ, *rad3*Δ *rad9*Δ, *rad3*Δ *hus1*Δ, *rad3*Δ *rad17*Δ, and *rad26*Δ *hus1*Δ all showed no additional telomere shortening compared to *rad3*Δ or *rad26*Δ single mutants (Figure 1B, lanes 10–17; Figure 2B). These results thus suggest that Rad1, Rad9, Hus1, Rad17, Rad3, and Rad26 contribute to telomere maintenance in a single pathway, but that Rad3 and Rad26 are more important in maintenance of telomeres in fission yeast.

Tel1 and Rad32 function in the same pathway for telomere maintenance: We next examined how checkpoint proteins interact with Tel1 and Rad32 proteins in *S. pombe*. Rad32 is an ortholog of the *S. cerevisiae* and mammalian Mre11 proteins. Studies in *S. cerevisiae* have shown that the Mre11-Rad50-Xrs2 complex and Tel1 function in a single pathway for telomere maintenance (Ritchie and Petes 2000; Tsukamoto *et al.* 2001).

We found that *tel1*Δ mutant cells had normal telomere length. We observed synergistic loss of telomeres in *tel1*Δ *rad3*Δ and *tel1*Δ *rad26*Δ cells (Figure 1C, lanes 7 and 8), in agreement with previous studies (Naito *et al.* 1998; Matsuura *et al.* 1999). Chromosome circularization in *tel1*Δ *rad3*Δ cells was previously reported, using PFGE analysis and microscopic observations (Naito *et al.* 1998), while chromosome circularization in *tel1*Δ *rad26*Δ cells has not been reported. As shown in Figure 3B, we observed that both *tel1*Δ *rad3*Δ and *tel1*Δ *rad26*Δ cells have fused C, I, L, and M *Not*I telomeric fragments to generate I + L and C + M bands that are specific to circularized chromosome I and chromosome II, respectively (lanes 7 and 8), like *trt1*Δ telomerase mutant survivors (lane 11; Nakamura *et al.* 1998). In contrast, other upstream checkpoint sensor mutants (*rad1*Δ, *rad9*Δ, *hus1*Δ, and *rad17*Δ) showed only slight telomere shortening compared to single mutants when combined with *tel1*Δ mutation (Figure 1C, lanes 3–6). Mutants of downstream effectors of the checkpoint pathway (*crb2*Δ, *chk1*Δ, *cds1*Δ, and *chk1*Δ *cds1*Δ) showed wild-type telomere length even in combination with a *tel1*Δ mutation (Figure 1C, lanes 9–12).

Rad32 mutant cells have previously been reported to have shorter than wild-type telomere length in *S. pombe* (Wilson *et al.* 1999; Manolis *et al.* 2001). We did not observe telomere shortening in our *rad32*Δ mutant (Figures 1D and 2D). Since *S. pombe* Rad32 and Rad50 are expected to be in a complex analogous to the *S. cerevisiae* Mre11-Rad50-Xrs2 complex, both mutations might be expected to show similar effects on telomere length. *S. pombe rad50*Δ cells have also been reported to have short telomeres (Hartsuiker *et al.* 2001). However, we observed normal telomere length for *rad50*Δ cells (data not shown), much like in *rad32*Δ cells. It was also suggested that *rad32*Δ mutation is synthetic lethal with *rad3* mutation (Tavassoli *et al.* 1995), but we were able to generate double mutants and propagate them for many generations, although these cells are extremely sick and produce many dead cells with abnormal morphology. We do not know the exact cause for these discrepancies, but unsuspected suppressor mutation(s) or variations in growth conditions might have contributed to these

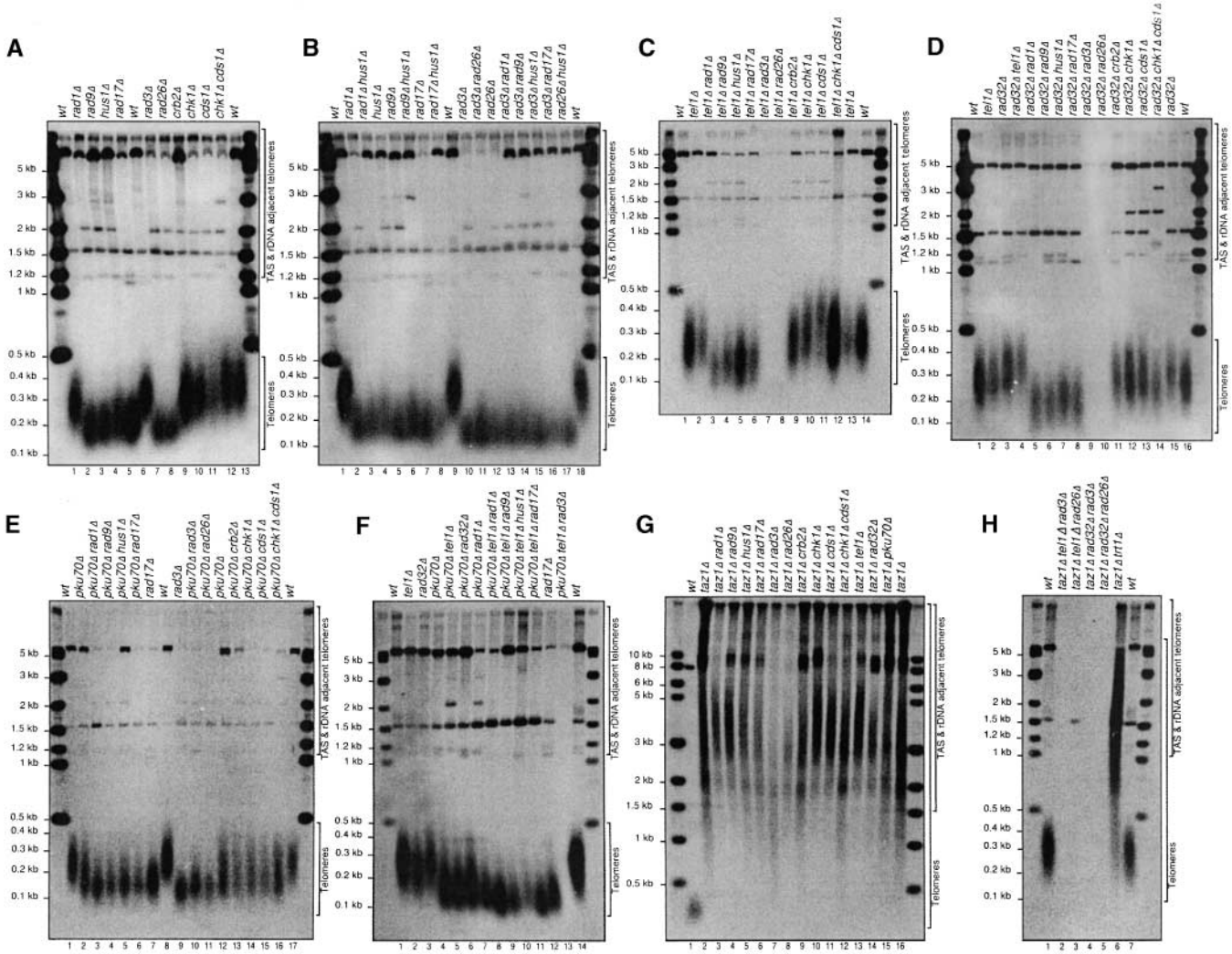

FIGURE 1.—Telomere lengths of various checkpoint-, DNA repair-, and telomere-related protein mutant combinations. After strains were created by either genetic crosses or DNA transformations, they were restreaked at least five times on YES plates prior to preparation of genomic DNA to ensure telomere length equilibrium. After digestion with *Apa*I, genomic DNA was subjected to electrophoresis on 2% (A–F and H) or 1% (G) agarose gels, stained with ethidium bromide to confirm approximately equal loading in each lane, transferred to a nylon membrane, and hybridized to a telomeric DNA probe (NAKAMURA *et al.* 1997). The *Apa*I site is located in the telomere-associated sequence (TAS) 30–40 bp away from telomeric repeat sequences in both ends of chromosomes I and II and at least one end of chromosome III (SUGAWARA 1988), giving rise to a broad ~300-bp telomere hybridization signal in the wild-type (wt) strain (marked as "telomeres"). Hybridization signals designated as "TAS & rDNA adjacent telomeres" come from cross-hybridization to TAS or hybridization to telomere(s) of chromosome III, which contain rDNA repeats directly adjacent to the telomeric repeat sequence and therefore lack the TAS-associated *Apa*I site directly adjacent to the telomeric repeat sequence.

disagreements. In this regard, we note that both *rad32*Δ and *rad50*Δ strains grow poorly and appear to accumulate DNA damage, as many cells appear to be arrested by the checkpoint.

When the *rad32*Δ mutation was combined with the *tel1*Δ mutation, we found that the *rad32*Δ *tel1*Δ double mutant still had normal telomere length (Figure 1D, lanes 1–4). When the *rad32*Δ mutation was combined with *rad1*Δ, *rad9*Δ, *hus1*Δ, or *rad17*Δ mutations, double mutants showed only slight shortening of telomere lengths compared to single mutants in *rad1*Δ, *rad9*Δ, *hus1*Δ, or *rad17*Δ strains (Figure 1D, lanes 5–8). Combination of the *rad32*Δ mutation with either *rad3*Δ or *rad26*Δ, on the other hand, caused total loss of the telomere hybridization signal (Figure 1D, lanes 9 and 10). This is due to circularization of chromosomes, as PFGE analysis showed a shift of C, I, L, and M telomeric *Not*I fragments into two bands corresponding to I + L and C + M bands (Figure 3B, lanes 9 and 10). Combination of the *rad32*Δ mutation and mutations of downstream effectors of the checkpoint pathway (*crb2*Δ, *chk1*Δ, *cds1*Δ, and *chk1*Δ *cds1*Δ) showed wild-type telomere length (Figure 1D, lanes 11–16). Therefore, *rad32*Δ and *tel1*Δ mutations caused identical phenotypes

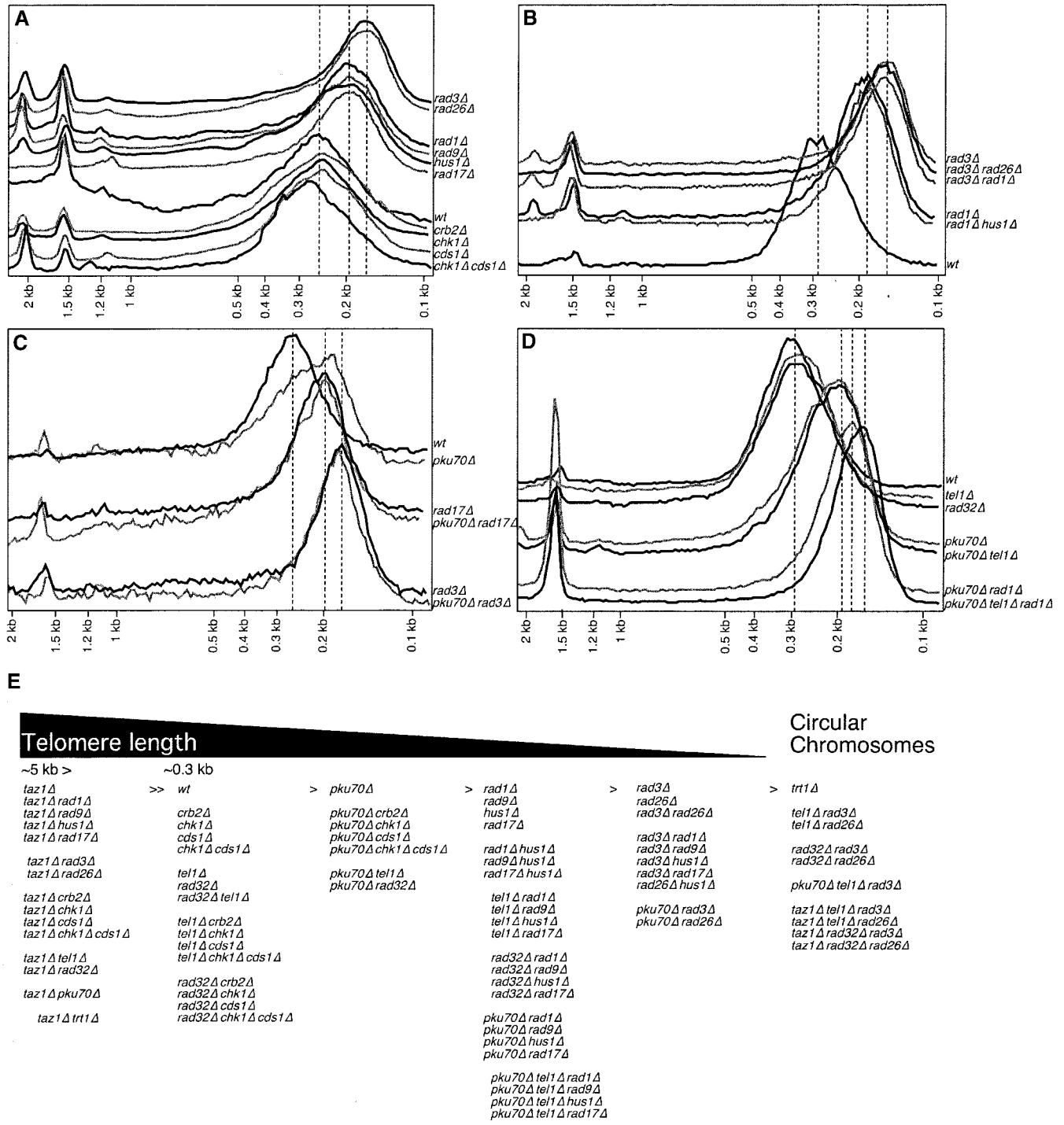

E

Telomere length

Circular Chromosomes

~5 kb > ~0.3 kb

taz1Δ >> wt > pku70Δ > rad1Δ > rad3Δ > trt1Δ

taz1Δ rad1Δ
taz1Δ rad9Δ
taz1Δ hus1Δ
taz1Δ rad17Δ

taz1Δ rad3Δ
taz1Δ rad26Δ

taz1Δ crb2Δ
taz1Δ chk1Δ
taz1Δ cds1Δ
taz1Δ chk1Δ cds1Δ

taz1Δ tel1Δ
taz1Δ rad32Δ

taz1Δ pku70Δ

taz1Δ trt1Δ

crb2Δ
chk1Δ
cds1Δ
chk1Δ cds1Δ

tel1Δ
rad32Δ
rad32Δ tel1Δ

tel1Δ crb2Δ
tel1Δ chk1Δ
tel1Δ cds1Δ
tel1Δ chk1Δ cds1Δ

rad32Δ crb2Δ
rad32Δ chk1Δ
rad32Δ cds1Δ
rad32Δ chk1Δ cds1Δ

pku70Δ crb2Δ
pku70Δ chk1Δ
pku70Δ cds1Δ
pku70Δ chk1Δ cds1Δ

pku70Δ tel1Δ
pku70Δ rad32Δ

rad9Δ
hus1Δ
rad17Δ

rad1Δ hus1Δ
rad9Δ hus1Δ
rad17Δ hus1Δ

tel1Δ rad1Δ
tel1Δ rad9Δ
tel1Δ hus1Δ
tel1Δ rad17Δ

rad32Δ rad1Δ
rad32Δ rad9Δ
rad32Δ hus1Δ
rad32Δ rad17Δ

pku70Δ rad1Δ
pku70Δ rad9Δ
pku70Δ hus1Δ
pku70Δ rad17Δ

pku70Δ tel1Δ rad1Δ
pku70Δ tel1Δ rad9Δ
pku70Δ tel1Δ hus1Δ
pku70Δ tel1Δ rad17Δ

rad26Δ
rad3Δ rad26Δ

rad3Δ rad1Δ
rad3Δ rad9Δ
rad3Δ hus1Δ
rad3Δ rad17Δ
rad26Δ hus1Δ

pku70Δ rad3Δ
pku70Δ rad26Δ

tel1Δ rad3Δ
tel1Δ rad26Δ

rad32Δ rad3Δ
rad32Δ rad26Δ

pku70Δ tel1Δ rad3Δ

taz1Δ tel1Δ rad3Δ
taz1Δ tel1Δ rad26Δ
taz1Δ rad32Δ rad3Δ
taz1Δ rad32Δ rad26Δ

FIGURE 2.—Phosphor-Imager analysis of telomere lengths for selected checkpoint and DNA repair mutants (A–D) and summary of telomere length analysis for all the mutant combinations tested in this study (E). Data from multiple Southern blots (Figure 1) were analyzed using ImageQuant software (Molecular Dynamics, Sunnyvale, CA) and signal intensities for telomere hybridization signals were normalized and plotted against DNA size. Graphs were shifted vertically to allow easier comparison of telomere lengths among different mutant cells. Dotted vertical lines indicate peaks of telomere hybridization signals.

in terms of telomere length in all checkpoint mutant backgrounds we tested. Taken together, these results are consistent with the idea that Tel1 and Rad32 function in the same pathway for telomere maintenance much like *S. cerevisiae* Tel1 and Mre11-Rad50-Xrs2. The above data also indicate that Rad3/Rad26 and Tel1/Rad32 represent two functional groups required for telomere maintenance in *S. pombe*.

Interaction between Ku70 and checkpoint proteins: Next, we tested how telomere length is affected by

combining the *pku70*Δ mutation with mutations in checkpoint genes *tel1*Δ and *rad32*Δ. In *S. pombe*, *pku70*Δ makes telomeres shorter and the telomere-associated sequences (TAS) more recombinogenic (Baumann and Cech 2000; Manolis *et al.* 2001). We observed shorter and more heterogeneous telomere length for *pku70*Δ cells compared to wild-type cells. We also found that double mutants of *pku70*Δ and checkpoint sensor protein mutations have the telomere lengths of checkpoint sensor single mutants for *rad1*Δ, *rad9*Δ, *hus1*Δ, *rad17*Δ, *rad3*Δ, and *rad26*Δ and also made telomere length more homogeneous compared to a *pku70*Δ strain (Figure 1E, lanes 1–11; Figure 2, C and D). Therefore, mutations in checkpoint sensor genes are epistatic to *pku70*Δ in maintenance of telomere length. For combinations of *pku70*Δ and downstream protein mutations (*crb2*Δ, *chk1*Δ, *cds1*Δ, and *chk1*Δ *cds1*Δ), telomere lengths were like that of the *pku70*Δ single mutant (Figure 1E, lanes 12–17). Telomere lengths in *pku70*Δ *tel1*Δ and *pku70*Δ *rad32*Δ cells were also the same as in the *pku70*Δ single mutant (Figure 1F, lanes 4–6; Figure 2D).

We also created triple mutants in which a checkpoint sensor was deleted along with *tel1*Δ and *pku70*Δ. We hypothesized that the Rad3-Rad26 complex may contribute positively to telomere maintenance both through a pathway involving Ku70 and through another pathway involving the Rad1/Rad9/Hus1/Rad17 proteins since mutations in *rad3* and *rad26* were found to be epistatic to mutations in *rad1*, *rad9*, *hus1*, *rad17*, and *pku70*. If this were true, deletion of both pathways in combination with the *tel1*Δ mutation might cause chromosomes to circularize as they do in *tel1*Δ *rad3*Δ or *tel1*Δ *rad26*Δ cells. However, we found that *pku70*Δ *tel1*Δ *rad1*Δ, *pku70*Δ *tel1*Δ *rad9*Δ, *pku70*Δ *tel1*Δ *hus1*Δ, and *pku70*Δ *tel1*Δ *rad17*Δ cells all maintained short but stable telomeres (Figure 1F, lanes 8–11). Telomere lengths in these triple-mutant cells were slightly reduced compared to single checkpoint mutant cells (*rad1*Δ, *rad9*Δ, *hus1*Δ, *rad17*Δ), *pku70*Δ checkpoint double-mutant cells (*pku70*Δ *rad1*Δ, *pku70*Δ *rad9*Δ, *pku70*Δ *hus1*Δ, *pku70*Δ *rad17*Δ), or *pku70*Δ *tel1*Δ cells (Figures 1F and 2D). PFGE analysis found no evidence of chromosome circularization in those triple-mutant cells (Figure 3C, lanes 2–5). Therefore, the Rad3-Rad26 complex must have additional telomere-associated targets, outside the Rad1/Rad9/Hus1/Rad17 and Ku70 epistasis groups, which confer protection from chromosome circularization in *tel1*Δ and *rad32*Δ backgrounds.

We also tested the possibility that synergistic chromosome circularization observed in *tel1*Δ *rad3*Δ cells might be suppressed by *pku70*Δ mutation. This might be the case because *pku70*Δ cells were reported to have elevated TAS recombination (Baumann and Cech 2000) and therefore loss of Ku70 protein might allow either the recombinational machinery or the telomerase better access to telomeres, thus suppressing the telomere loss

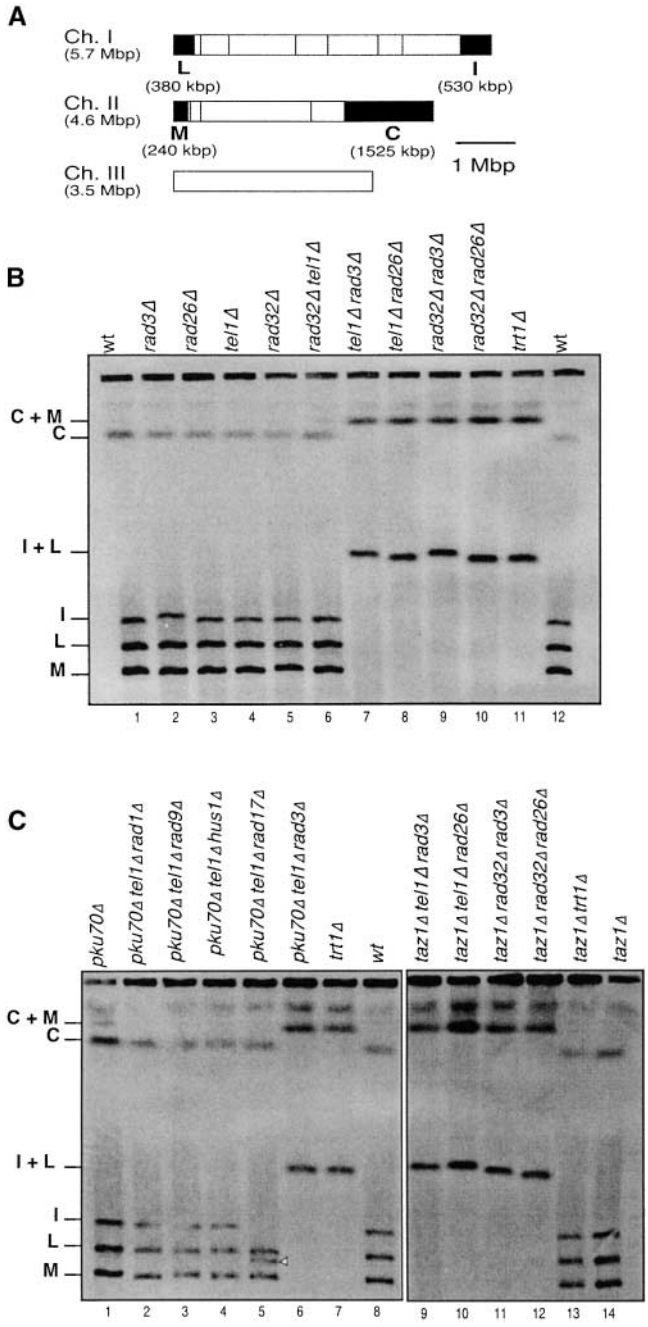

Figure 3.—Pulsed-field gel electrophoresis fractionation and hybridization analysis of *S. pombe* chromosomal DNAs. (A) *Not*I restriction enzyme map of *S. pombe* chromosomes (vertical lines). The telomeric fragments C, I, L, and M are solid. Chromosome III lacks a *Not*I site. (B and C) *Not*I-digested *S. pombe* chromosomal DNAs were fractionated in a 1% agarose gel with 0.5× TBE buffer at 14°, using the CHEF-DR II system (Bio-Rad) at 6 V/cm (200 V) and a pulse time of 60–120 sec for 24 hr, transferred to nylon membrane, and hybridized to C-, I-, L-, and M-specific probes (Nakamura *et al.* 1998). Four telomeric fragments (C, I, L, and M) and fusion products (C + M and I + L) are marked on the left. The "I" fragment from *pku70*Δ *tel1*Δ *rad17*Δ cells migrates faster (marked with a triangle) since the *rad17*$^+$ gene resides on the I fragment and the deletion mutation introduced an additional *Not*I site.

observed in the *tel1*Δ *rad3*Δ background. Alternatively, the Rad3 and Tel1 kinase pathways may be necessary to specifically inhibit the NHEJ pathway from fusing chromosome ends. In that case, elimination of NHEJ by removal of Ku protein may allow cells to avoid fusing their telomeres. Indeed, telomere fusions observed in nitrogen-starved *taz1*Δ cells can be suppressed by *pku70*Δ or *lig4*Δ mutation (Ferreira and Cooper 2001). However, *pku70*Δ *tel1*Δ *rad3*Δ cells again completely lost telomeric hybridization (Figure 1F, lane 13) and have circular chromosomes (Figure 3C, lane 6). Therefore, *pku70*Δ mutation cannot suppress chromosome circularization in *tel1*Δ *rad3*Δ cells.

Interaction between Taz1 and checkpoint proteins: In *S. cerevisiae*, the telomere shortening phenotype of a *tel1* mutation is epistatic over the telomere elongation phenotype of the *rap1-17* mutation (Craven and Petes 1999; Ray and Runge 1999). Rap1 is a major telomere-binding protein in *S. cerevisiae*, and Rap1, through interaction with the Rif1 and Rif2 proteins, is thought to be involved in negative regulation of telomerase activity and telomeric recombination (Hardy *et al.* 1992; Wotton and Shore 1997). Rap1 interacts with Rif1 and Rif2 through its carboxy-terminal domain, and the *rap1-17* mutation disrupts these associations. The fact that the *tel1*Δ *rap1-17* double mutant has a short telomere length, much like the *tel1*Δ mutant, suggests that in *S. cerevisiae* telomerase recruitment/activation is still largely dependent on Tel1 kinase even in the absence of negative regulators of telomerase (Craven and Petes 1999; Ray and Runge 1999).

As deletion of *S. pombe* Taz1 telomere-binding protein leads to extreme elongation of the telomere tract, which is reminiscent of the *S. cerevisiae rap1-17* phenotype (Cooper *et al.* 1997), we tested whether telomere elongation in *taz1*Δ required Tel1, Rad32, Ku70, or other checkpoint proteins. We created double-mutant combinations by individually deleting the *taz1* gene from single-mutant cells of *rad1*Δ, *rad9*Δ, *hus1*Δ, *rad17*Δ, *rad3*Δ, *rad26*Δ, *crb2*Δ, *chk1*Δ, *cds1*Δ, *chk1*Δ *cds1*Δ, *tel1*Δ, *rad32*Δ, and *pku70*Δ. We used this sequential procedure to eliminate the possibility that starting with highly elongated *taz1*Δ telomeres would mask the effects of the checkpoint mutations. The resulting double-mutant cells were then restreaked multiple times on rich media to allow cells to achieve equilibrium telomere length. As shown in Figure 1G, we found that telomeres are still elongated in all double-mutant cells. In *taz1*Δ *rad3*Δ and *taz1*Δ *rad26*Δ, telomere elongation was slightly reduced compared to *taz1*Δ cells, but they were still extremely elongated compared to wild-type telomere length (Figure 1G, lanes 1, 7, and 8). These results indicate that telomere elongation in the *taz1*Δ mutant is epistatic to mutations in the Tel1/Rad32, checkpoint sensors (Rad1/Rad9/Hus1/Rad17 and Rad3/Rad26), or Ku70 epistasis groups.

If telomere elongation in *taz1*Δ cells is independent of Tel1 and Rad3 kinases, the elongation induced by the *taz1* deletion might be expected to suppress the rapid telomere loss and circularization of *tel1*Δ *rad3*Δ cells. To test this possibility, we also created *taz1*Δ *tel1*Δ *rad3*Δ, *taz1*Δ *tel1*Δ *rad26*Δ, *taz1*Δ *rad32*Δ *rad3*Δ, and *taz1*Δ *rad32*Δ *rad26*Δ cells. These triple-mutant strains were created by deleting the *tel1* or *rad32* gene from the *taz1*Δ *rad3*Δ or *taz1*Δ *rad26*Δ cells. Therefore, these cells originally had highly elongated telomeres prior to the deletions. We found that the triple-mutant cells still completely lost their telomere hybridization signal (Figure 1H, lanes 2–5) and circularized their chromosomes (Figure 3C, lanes 9–12), indicating that even in the absence of Taz1 protein, telomeres cannot be maintained in *tel1*Δ *rad3*Δ, *tel1*Δ *rad26*Δ, *rad32*Δ *rad3*Δ, or *rad32*Δ *rad26*Δ backgrounds. In contrast, chromosome circularization observed in telomerase *trt1*Δ mutants (Figure 3B, lane 11) was suppressed and the cells maintained stable linear chromosomes indefinitely if the *trt1* gene was deleted in cells that were already deleted for *taz1* (Figure 1H, lane 6; Figure 3C, lane 13; Nakamura *et al.* 1998). In *taz1*Δ *trt1*Δ cells, telomeres are presumably maintained by recombination (Nakamura *et al.* 1998). Therefore, the fact that the *taz1*Δ mutation could not overcome elimination of the Rad3/Rad26 and Tel1/Rad32 pathways suggests that these pathways are necessary for both telomerase-based and recombination-based maintenance of telomeres.

Rad3 and Tel1 kinases have additional roles other than recruitment of telomerase: In *S. pombe*, careful analysis of how *tel1*Δ or checkpoint mutants affect the rate of senescence in telomerase mutant cells has not yet been carried out, nor has direct comparison of the rate of senescence for telomerase *vs. tel1*Δ *rad3*Δ mutants. Therefore, we undertook such analyses to gain insight into the contribution of Rad3/Rad26 and Tel1/Rad32 pathways to telomere maintenance.

We performed a series of growth curve experiments in which heterozygous diploid cells were sporulated and dissected, and then cultures of cells with appropriate genotypes were serially diluted (Figure 4). As previously reported (Nakamura *et al.* 1998; Haering *et al.* 2000), the growth rate of *trt1*Δ cells gradually declined in a reproducible manner from day 2 to day 10 in independent liquid cultures (Figure 4A and data not shown). On the other hand, different *trt1*Δ cultures displayed different patterns of recovery in growth rate in the phase when survivor cells start to take over the cultures. We did not observe a delayed decline in growth rate for *tel1*Δ *trt1*Δ cells compared to *trt1*Δ cells (Figure 4B). For *rad3*Δ *trt1*Δ and *rad26*Δ *trt1*Δ cells, the rate at which growth rates declined among independent cultures became much less reproducible compared to *trt1*Δ cells (Figure 4, C and D). This effect presumably is related to the checkpoint-related functions of Rad3 and Rad26, as *chk1*Δ *trt1*Δ cells showed similarly wide-ranging vari-

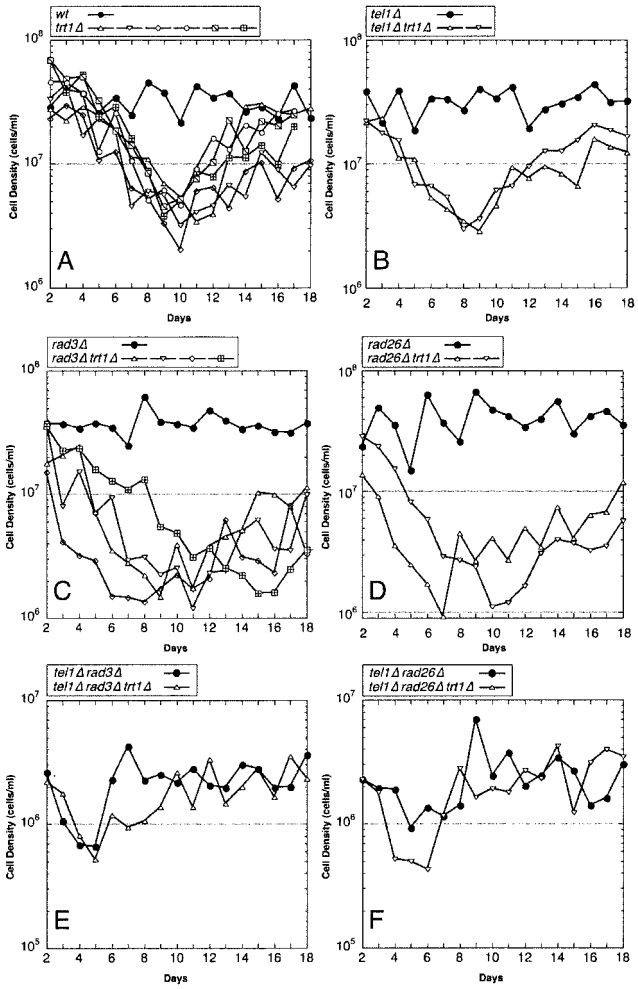

FIGURE 4.—Comparison of growth characteristics of wild-type (*wt*) and mutant cells after extended growth in liquid cultures. Various heterozygous diploid strains (see the supplementary Table S1 at http://www.genetics.org/supplemental) were sporulated and the resulting tetrads were dissected and germinated on YES plates. The resulting haploid cells with indicated genotypes were grown at 32° for 3 days and then picked and diluted to 5×10^4 cells/ml in YES. These cultures were grown for 24 hr at 32°, at which point the cell density was determined, and the cells were diluted into fresh YES liquid medium at 5×10^4 cells/ml. These procedures were repeated for 18 days, and cell densities from each day were plotted (see MATERIALS AND METHODS for more detailed procedures).

ability in decline of growth rate among independent cultures (data not shown).

As *trt1*Δ cells undergo senescence, an increasingly large fraction of cells becomes highly elongated (NAKAMURA *et al.* 1997). These elongated cells were not observed in *rad3*Δ *trt1*Δ, *rad26*Δ *trt1*Δ, or *chk1*Δ *trt1*Δ cells, suggesting that senescing *trt1*Δ cells show checkpoint-dependent cell cycle arrest as the cells lose their telomeric DNA (data not shown). Interestingly, *cds1*Δ *trt1*Δ cells still elongated as they senesced, and growth rate decline was similar to that in *trt1*Δ cells and without wide-ranging variations among independent cultures (data not shown). Therefore, defective telomeres in *trt1*Δ cells appear to be recognized as DSBs and trigger G2 checkpoint cell cycle arrest.

We next compared growth characteristics among *tel1*Δ *rad3*Δ, *tel1*Δ *rad3*Δ *trt1*Δ, *tel1*Δ *rad26*Δ, and *tel1*Δ *rad26*Δ *trt1*Δ cells after germination of meiotic spores from heterozygous diploid cells. We observed that both *tel1*Δ *rad3*Δ and *tel1*Δ *rad26*Δ reached the point of lowest viability much earlier (~5 days) than *trt1*Δ cells did (~10 days), and survivors grew more slowly than *trt1*Δ survivor cells (Figure 4, E and F). Moreover, *tel1*Δ *rad3*Δ *trt1*Δ and *tel1*Δ *rad26*Δ *trt1*Δ cells did not show any additional loss of growth rate compared to *tel1*Δ *rad3*Δ and *tel1*Δ *rad26*Δ. Therefore, the presence of functional telomerase did not help to delay senescence. The accelerated senescence phenotype observed for *tel1*Δ *rad3*Δ and *tel1*Δ *rad26*Δ cells is reminiscent of those seen in *pku70*Δ *trt1*Δ cells and cells lacking the proposed telomere capping protein, Pot1 (BAUMANN and CECH 2000, 2001). Therefore, the two pathways involving Rad3/Rad26 and Tel1/Rad32 must play roles not only in telomerase recruitment, but also in other functions such as telomere protection.

Phosphorylation of Rad32 is independent of Rad3 and Tel1: Previous studies have shown that Rad32 is phosphorylated in a cell-cycle-dependent manner. Rad32 phosphorylation accumulates in S-phase and this phosphorylation is independent of Rad3 (WILSON *et al.* 1998). Our genetic analysis indicated that Rad32 and Tel1, but not Rad3, function in the same pathway to maintain telomere length in fission yeast. Therefore, we tested whether Rad32 phosphorylation might be crucial for Rad32 telomere function and whether Tel1 might be responsible for Rad32 phosphorylation.

Rad32 phosphorylation was detected by the appearance of a slow mobility species in SDS-PAGE that can be converted to a faster mobility species by treatment with phosphatase (Figure 5A). Asynchronous *S. pombe* cells showed a small amount of Rad32 phosphorylation, which is probably due to a small percentage of cells that are in S-phase (Figure 5B). In contrast, when cells were arrested in S-phase through the addition of hydroxyurea (HU) or when cells were exposed to the DNA-damaging agent methyl methanesulfonate (MMS), increased phosphorylation of Rad32 was observed. Phosphorylation of Rad32 was still observed in *rad1*Δ, *rad9*Δ, *hus1*Δ, *rad17*Δ, *crb2*Δ, *chk1*Δ, *cds1*Δ, and *chk1*Δ *cds1*Δ cells (data not shown) and, surprisingly, in *tel1*Δ, *tel1*Δ *rad3*Δ (Figure 5B), and *tel1*Δ *rad26*Δ cells (data not shown). These results showed that Rad3 and Tel1 are not the kinases responsible for the observed Rad32 phosphorylation and suggest that there must be other kinase(s) that can phosphorylate Rad32. However, it is possible that Rad3 or Tel1 carries out phosphorylation of Rad32 that does not alter its mobility on SDS-PAGE. Whether Rad32 phosphorylation is actually required to maintain telomeres has to be resolved. We observed more prominent

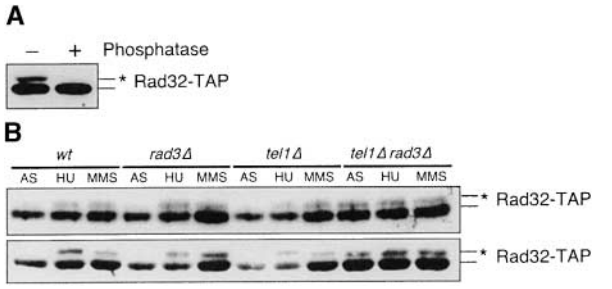

FIGURE 5.—Rad32 phosphorylation is independent of Rad3 and Tel1. (A) TAP-tagged Rad32 was affinity purified from asynchronous *rad32-TAP* cells. Purified Rad32-TAP was either mock treated or phosphatase treated prior to Western blot analysis. (B) Wild-type (*wt*), *rad3*Δ, *tel1*Δ, and *rad3*Δ *tel1*Δ cells with *rad32-TAP* were either treated with 12 mM HU or 0.05% MMS for 3 hr or left untreated (AS). Extracts were prepared from these cells and Rad32-TAP affinity purifications were performed. Whole-cell extracts (top) and affinity-purified protein (bottom) were analyzed by immunoblotting. (*) phosphorylated form of Rad32-TAP.

phosphorylation of Rad32 in asynchronous *tel1*Δ *rad3*Δ and *tel1*Δ *rad26*Δ cells (Figure 5B and data not shown). These cells are extremely sick and have circular chromosomes (Figure 3B, lanes 7 and 8). We suggest that these cells have problems in either DNA replication or DNA segregation and therefore accumulate DNA damage, which may explain why these cells have elevated Rad32 phosphorylation.

Checkpoint sensor and DNA repair proteins are bound to telomeric DNA: Recent studies in *S. cerevisiae* showed that Mec1, Ddc2, Rad24, Rad17, Ddc1, and Mec3 (homologs of *S. pombe* Rad3, Rad26, Rad17, Rad1, Rad9, and Hus1, respectively) are recruited to sites of DNA breaks upon induced DNA damage (KONDO *et al.* 2001; MELO *et al.* 2001; ROUSE and JACKSON 2002). Therefore, we tested if the checkpoint sensor proteins are physically bound to normal telomeres by performing ChIP assays. As controls we chose the known telomere-binding protein Taz1. Telomeric binding of Taz1 *in vivo* by ChIP assay has been reported recently (KANOH and ISHIKAWA 2001). We also tested telomeric binding of Ku70 by ChIP assay. Binding of Ku proteins to telomeres has been established in mammals and *S. cerevisiae* (GRAVEL *et al.* 1998; HSU *et al.* 1999, 2000; D'ADDA DI FAGAGNA *et al.* 2001). On the other hand, binding of the *S. pombe* Ku70 to telomeres has not been investigated directly, and a recent report showed that *S. pombe* Ku70 is localized throughout the nucleus and not confined to telomeres (MANOLIS *et al.* 2001). Precipitated DNA was amplified by PCR with primers for the telomere-associated sequence TAS (Figure 6A) and the non-telomere-adjacent *ade6*$^+$ gene. Telomeric DNA, but not *ade6*$^+$ DNA, was specifically amplified from Taz1-HA, Ku70-HA, and Ku70-myc immunoprecipitates while no such enrichment was observed for a nontagged strain (Figure 6, B and C). This result shows specific binding of Ku protein to telomeres in fission yeast.

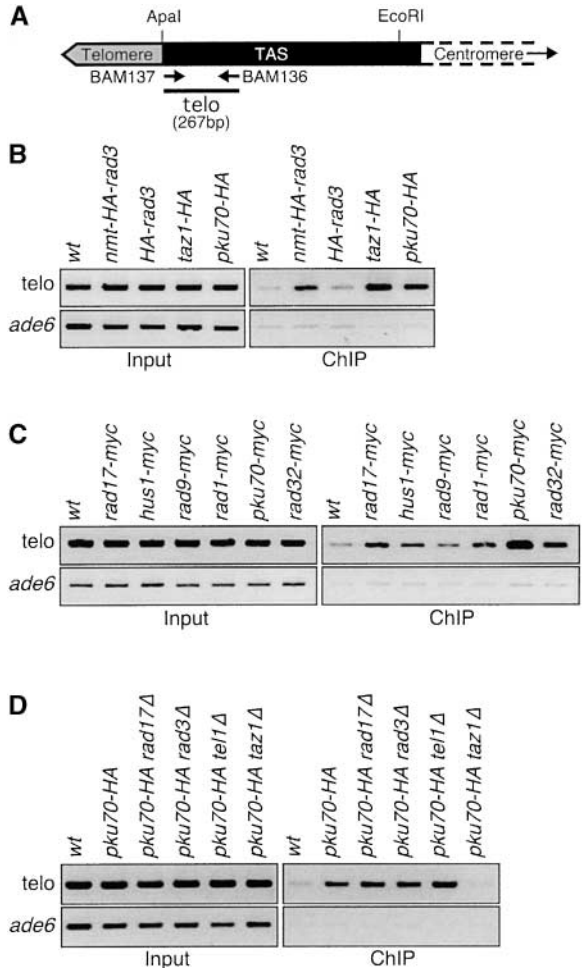

FIGURE 6.—Checkpoint sensor proteins Rad32 and Ku70 bind to telomeres *in vivo*. (A) Schematic diagram of the *S. pombe* telomere and TAS region. Primers used in the ChIP assay are indicated. (B) ChIP assay of Rad3, Taz1, and Ku. Untagged wild-type control strain or strains with indicated HA-tagged proteins were used. (C) ChIP assay of Rad17, Hus1, Rad9, Rad1, Ku70, and Rad32. Untagged wild-type control strain or strains with indicated myc-tagged proteins were used. (D) ChIP assay of Ku70 in various deletion strains. Untagged wild-type control strain and strains with *pku70-HA* in indicated mutant backgrounds were used. PCRs were performed on whole-cell extracts (Input) and on chromatin immunoprecipitates (ChIP) using primers to amplify a telomere-specific DNA (telo) and primers to amplify DNA from the *ade6*$^+$ gene (*ade6*).

We were unable to detect HA-Rad3 at the telomere when it was expressed from its endogenous promoter, possibly because of its low abundance. On the other hand, HA-Rad3 overexpressed from the *nmt* promoter was able to specifically enrich telomeric DNA, but not the control *ade6*$^+$ DNA, suggesting that Rad3 binds specifically to telomeres (Figure 6B). However, we cannot exclude the possibility that overexpressed Rad3 associates with telomeres in a nonphysiological manner. We also observed enrichment of telomeric DNA over *ade6*$^+$ DNA in immunoprecipitates from Rad17-myc and to a lesser extent from Rad1-myc, Rad9-myc, and Hus1-myc (Figure 6C). Although the signals we obtained were

weaker than those for Ku70-myc, they were reproducible. Differences in signal intensity are most likely due to differences in immunoprecipitation efficiency and protein abundance at the telomere. Taken together, these ChIP assays show that Rad3 and Rad17 and most likely Rad1, Rad9, and Hus1 bind to telomeres. We also obtained a low, but significant signal for telomeric DNA in immunoprecipitates from Rad32-myc cells (Figure 6B). Therefore, our data show that Rad32 also binds to telomeres.

Ku70 binding to telomeric DNA is independent of checkpoint sensor proteins but dependent on Taz1 protein: In our genetic analysis we found that the mutations eliminating checkpoint sensor proteins are epistatic to *pku70*Δ in maintaining stable telomere length, indicating that these proteins may function in the same pathway. To investigate whether Ku70 binding to telomeres might be dependent on the checkpoint sensor proteins, we undertook ChIP analyses (Figure 6D). We observed no change in Ku70 binding in either *rad17*Δ or *rad3*Δ mutants, indicating that the checkpoint sensor proteins do not function through regulating binding of Ku70 to telomeres.

We also investigated Ku70 binding to telomeres in *tel1*Δ and *taz1*Δ mutants. Again, no change in telomere binding was found in the *tel1*Δ strain. In contrast, in the absence of Taz1 protein, Ku70 binding was greatly diminished. This datum is consistent with data from mammalian cells in which Ku70 is found to bind the Taz1 homologs TRF1 and TRF2 (Hsu *et al.* 2000; Song *et al.* 2000), and Ku heterodimers can be recruited to the circular DNA with internal telomeric repeat sequence via their association with TRF1 (Hsu *et al.* 2000). Our data may therefore indicate that Ku70 binding to telomeres is facilitated through Taz1. However, we cannot exclude the possibility that Ku70 binds exclusively to the very termini of chromosomes and that the apparent loss of Ku70 binding is caused by telomere elongation in *taz1*Δ cells, since our ChIP assay is designed to detect proteins bound to sites close to TAS (~500–1000 bp).

DISCUSSION

Checkpoint sensor proteins have alternative targets for telomere maintenance: In this study, we extensively tested the relative contributions of *S. pombe* checkpoint and DNA repair proteins in telomere maintenance by creating cells carrying various mutant combinations and examining average telomere length and chromosome circularization in the resulting cells. Our results are summarized in Figure 2E. One of the conclusions we draw from such analyses is that downstream effectors of the checkpoint (Crb2, Chk1, and Cds1) are not important for telomere maintenance in *S. pombe*, even though checkpoint sensor proteins (Rad1, Rad9, Hus1, Rad17, Rad3, and Rad26) are required for proper telomere maintenance. Therefore, checkpoint sensor proteins must contribute to telomere maintenance through alternative telomere target(s) that are unrelated to these checkpoint effectors.

Previous studies in *S. pombe* also found Chk1 and Cds1 to be not important for telomere maintenance (Dahlén *et al.* 1998; Matsuura *et al.* 1999). On the other hand, one study suggested Crb2 is important for telomere maintenance since *crb2*Δ (*rhp9*Δ) cells have shorter telomere length (Wilson *et al.* 1999). We do not know the cause of this discrepancy, but we note that our *crb2*Δ strains are generated by backcrossing a *crb2*Δ strain obtained from a laboratory different (Saka *et al.* 1997) from that of the study that reported telomere shortening in *crb2*Δ cells. In comparison, *S. cerevisiae rad53* (*S. pombe* Cds1 homolog) mutants have been reported to have short telomeres (Longhese *et al.* 2000), while *S. cerevisiae rad9*Δ (*S. pombe* Crb2 homolog) cells were variously reported to have short (Vialard *et al.* 1998) or wild-type (Longhese *et al.* 2000) telomere length.

Checkpoint sensors Rad1, Rad9, Hus1, and Rad17 function in a single pathway for telomere maintenance and associate with telomeres: Our studies indicate that checkpoint proteins with PCNA homology (Rad1, Rad9, and Hus1) as well as the RFC-like protein Rad17, which has been proposed to recruit the Rad1-Rad9-Hus1 complex to sites of DNA damage, function in the same pathway for maintenance of telomere length. This conclusion is based on the observation that mutant combinations among these proteins did not lead to additional telomere shortening and mutants lacking these four proteins showed identical telomere lengths under all different mutant backgrounds (*tel1*Δ, *rad32*Δ, *pku70*Δ, *pku70*Δ *tel1*Δ, *taz1*Δ) that we tested.

Our results are consistent with results from previous studies for *rad1* and *rad17* mutants (Dahlén *et al.* 1998; Matsuura *et al.* 1999). However, our results disagree with a previous study for *rad9* and *hus1* mutants where *S. pombe rad9-192* and *hus1*Δ mutations were found not to affect telomere length (Dahlén *et al.* 1998). Since the previous study tested telomere length in *rad9-192* cells and not *rad9*Δ cells, the difference between the two results may be explained by partial retention of function of the *rad9-192* allele with respect to telomere length maintenance, although *rad9-192* is as sensitive to UV and ionizing radiation as a *rad9*Δ mutant strain (Murray *et al.* 1991; Lieberman *et al.* 1992). On the other hand, the previous study and our study used the same *hus1::LEU2* deletion mutation; this latter disagreement cannot be easily explained.

In *S. cerevisiae*, *rad17*Δ (*S. pombe rad1* homolog) and *ddc1*Δ (*S. pombe rad9* homolog) cells were reported to have short telomeres, and they were considered to be in the same pathway, since *rad17*Δ *ddc1*Δ double-mutant cells showed no additional telomere shortening (Longhese *et al.* 2000). Curiously, *S. cerevisiae mec3*Δ cells (*S. pombe hus1* homolog) were reported to have longer (Corda *et al.* 1999; Longhese *et al.* 2000) or wild-type (Grandin *et al.* 2001) telomere length. Therefore, checkpoint proteins with the PCNA-like motif may not

have completely equivalent functions in *S. cerevisiae*. It is also interesting to note that *S. cerevisiae rad24*Δ (*S. pombe rad17* homolog) was reported to have wild-type telomere length (Longhese *et al.* 2000) even though it was recently shown that Rad24 was necessary to recruit Ddc1 to sites of DNA DSBs (Kondo *et al.* 2001; Melo *et al.* 2001).

Our ChIP analyses showed robust binding of *S. pombe* Rad17 to telomeres, while the PCNA-like checkpoint proteins (Rad1, Rad9, and Hus1) bound weakly. Therefore, we suggest that the checkpoint proteins with RFC and PCNA homology contribute to telomere maintenance through their binding to telomeres. As telomere shortening in this class of checkpoint proteins is also observed in *S. cerevisiae* and *C. elegans* (Ahmed and Hodgkin 2000; Longhese *et al.* 2000), we suggest that this is a highly conserved mechanism. Perhaps PCNA-like checkpoint proteins may provide a launching pad for recruitment of factors that help prepare telomeres to be extended by telomerase, which is analogous to PCNA-dependent recruitment of DNA replication proteins.

The Rad3-Rad26 complex has additional roles that are independent of other checkpoint sensor proteins and that function through its association with telomeres: Our data indicated that Rad3 kinase and its proposed regulatory subunit Rad26 together form a separate epistasis group for telomere maintenance from other checkpoint sensor proteins, as these two proteins had the shortest telomere lengths among checkpoint sensor proteins and the *rad3*Δ *rad26*Δ double-mutant cells had the same telomere length as single-mutant cells. Studies by other groups also found similar results for *rad3*Δ and *rad26*Δ mutants (Dahlén *et al.* 1998; Matsuura *et al.* 1999). In addition, *rad3*Δ and *rad26*Δ mutant cells behaved in an identical manner when they were combined with *hus1*Δ, *tel1*Δ, *rad32*Δ, *pku70*Δ, *taz1*Δ, *tel1*Δ *taz1*Δ, and *rad32*Δ *taz1*Δ mutations, and thus these data also support the idea that Rad3 and Rad26 proteins function in the same pathway.

We found that Rad1/Rad9/Hus1/Rad17 and Rad3/Rad26 epistasis groups contribute to telomere maintenance in a single pathway. This conclusion was reached because double mutants, which carry one mutation from the Rad1/Rad9/Hus1/Rad17 group and another mutation from the Rad3/Rad26 group, behaved like the single mutants in the Rad3/Rad26 group. A previous report also showed that *rad1-1 rad3*Δ and *rad17w rad3*Δ cells have the same telomere length as *rad3*Δ cells (Matsuura *et al.* 1999). It is noteworthy that only *rad3*Δ and *rad26*Δ mutants, but not *rad1*Δ, *rad9*Δ, *hus1*Δ, and *rad17*Δ mutants, showed a synergistic chromosome circularization phenotype when they were combined with a *tel1*Δ or *rad32*Δ mutation. Therefore, Rad3/Rad26 must have additional unidentified targets other than Rad1/Rad9/Hus1/Rad17 that are important for telomere maintenance.

Ku70 was found to represent an additional epistasis group, which, in addition to Rad1/Rad9/Hus1/Rad17, acts in the Rad3/Rad26 pathway because telomere shortening phenotypes exhibited by *rad3*Δ and *rad26*Δ mutants were epistatic to that of the *pku70*Δ mutation. Therefore, it was possible that Ku70 by itself or together with Rad1/Rad9/Hus1/Rad17 might represent the critical telomere targets of the Rad3/Rad26 pathway that allow cells to maintain telomere in the absence of Tel1 or Rad32. However, cells simultaneously lacking the Tel1/Rad32, Rad1/Rad9/Hus1/Rad17, and Ku70 pathways maintained short but stable telomeres. Therefore, Rad3/Rad26 must have additional telomere targets besides Rad1/Rad9/Hus1/Rad17 and Ku70.

The list of proteins postulated to be phosphorylated by *S. pombe* Rad3, *S. cerevisiae* Mec1, and the mammalian counterpart ATR and ATM kinases is vast and includes RFC- and PCNA-related checkpoint proteins, RPA, and mammalian telomere-binding protein TRF1 (*S. pombe* Taz1 homolog; Paciotti *et al.* 1998; Brush and Kelly 2000; Bao *et al.* 2001; Kishi *et al.* 2001; Oakley *et al.* 2001; Post *et al.* 2001; Wang *et al.* 2001). It will be a challenge in the future to determine what is regulated by Rad3/Rad26 and crucial for telomere maintenance.

We observed that Rad3 binds specifically to telomeric DNA when overexpressed. Recent studies in *S. cerevisiae* suggest that the Mec1-Ddc2 complex (*S. pombe* Rad3-Rad26 homolog) binds specifically to sites of DNA DSBs (Kondo *et al.* 2001; Melo *et al.* 2001; Rouse and Jackson 2002). Therefore, our data showing specific binding of Rad3, Rad17, and Rad1-Rad9-Hus1 complexes to telomeres support the notion that checkpoint sensor proteins actually recognize functional telomeres as DNA DSBs. Checkpoint sensor proteins may thus recruit and regulate factors important for telomere maintenance through their physical association with telomeres.

Tel1 and Rad32 function in a single pathway for maintenance of telomeres, yet Rad32 phosphorylation is independent of Tel1 kinase: In this study, we established that Tel1 kinase and Rad32 (Mre11 ortholog) are in the same functional group and that the Tel1/Rad32 pathway is essential for preventing *rad3*Δ or *rad26*Δ mutant cells from losing telomeres. Therefore, Rad3/Rad26 and Tel1/Rad32 pathways represent two independent pathways required for telomere maintenance in *S. pombe*.

In *S. cerevisiae*, the Mre11-Rad50-Xrs2 complex and Tel1 function in a single pathway for telomere maintenance, and combining a *mec1* mutation with mutations in the Tel1/Mre11/Rad50/Xrs pathway causes telomere shortening and senescence (Ritchie *et al.* 1999; Ritchie and Petes 2000; Tsukamoto *et al.* 2001). Therefore, the synergistic phenotype reminiscent of the telomerase-negative phenotype observed in double mutants of ATR- and ATM-related kinases is conserved between *S. cerevisiae* and *S. pombe*. In addition, *S. cerevisiae* Mre11 and *S. pombe* Rad32 appear to function in the

same pathway as Tel1 for maintenance of telomeres in both organisms. However, it should be noted that between *S. cerevisiae* and *S. pombe*, the Tel1 and the Rad3 (*S. cerevisiae* Mec1) pathways seem to differ in importance. In *S. cerevisiae*, telomere length is much shorter in *tel1* mutants than in *mec1* mutants (Ritchie *et al.* 1999; Chan *et al.* 2001). On the other hand, in *S. pombe*, *tel1*Δ and *rad32*Δ cells have essentially normal telomere length while *rad3*Δ and *rad26*Δ cells have short telomeres.

In *S. cerevisiae*, Mre11 phosphorylation is induced in response to DNA damage. This phosphorylation is largely independent of Mec1, but dependent on Tel1 (D'Amours and Jackson 2001; Usui *et al.* 2001). In addition, Tel1-dependent phosphorylation of Xrs2 in *S. cerevisiae* (D'Amours and Jackson 2001; Usui *et al.* 2001) and ATM (Tel1 homolog)-dependent phosphorylation of Nbs1 (Xrs2 homolog) in mammalian cells (Gatei *et al.* 2000; Lim *et al.* 2000) were reported. These data suggest that phosphorylation of the Mre11-Rad50-Xrs2 complex by Tel1 kinase or phosphorylation of the Mre11-Rad50-Nbs1 complex by ATM kinase plays an important role in telomere maintenance.

In light of these findings, we tested if Rad32 phosphorylation was dependent on Tel1 and Rad3 kinases in fission yeast. To our surprise, neither kinase appears to be required for Rad32 phosphorylation, as judged by the mobility shift of Rad32. Therefore, our data suggest that unknown kinase(s) other than Rad3 and Tel1 are responsible for Rad32 phosphorylation and that Rad32 phosphorylation is not sufficient for telomere maintenance. This unknown kinase cannot be Chk1 or Cds1 because we observed Rad32 phosphorylation in *chk1*Δ *cds1*Δ cells (data not shown).

A ChIP assay indicated that Rad32 is bound to telomeres. This result thus suggests that Rad32 protein contributes to telomere length maintenance as part of telomere chromatin in *S. pombe*. Immunofluorescence studies in human cells showed that the Mre11-Rad50-Nbs1 complex is associated with telomeres (Lombard and Guarente 2000; Zhu *et al.* 2000). Therefore, binding of the Mre11-Rad50-related complex to telomeres is conserved in both *S. pombe* and humans and is likely to occur in other species as well.

Cells lacking Rad3/Rad26 and Tel1/Rad32 pathways have defects in addition to recruitment of telomerase: We found that the *taz1*Δ mutation cannot suppress chromosome circularization caused by simultaneous inactivation of Rad3/Rad26 and Tel1/Rad32 pathways. These results suggest that telomere defects in these cells cannot be due solely to an inability to recruit telomerase because the *taz1*Δ mutation can suppress the chromosome circularization phenotype of a telomerase *trt1*Δ mutation. We also observed chromosome circularization in *taz1*Δ *tel1*Δ *rad3*Δ *trt1*Δ quadruple-mutant cells (data not shown). Therefore, the presence of telomerase was not the reason why *taz1*Δ *tel1*Δ *rad3*Δ cells circularized their chromosomes.

These results surprised us, as it was recently found in *S. cerevisiae* that the senescence phenotype observed in *tel1 mec1* double-mutant cells can be suppressed by additional mutations in telomere proteins such as Rif1 and Rif2 or alternations of telomere sequence, which affect the binding of Rap1 (Chan *et al.* 2001). On the other hand, *taz1*Δ cells seem to be defective in some aspects of telomere capping (Ferreira and Cooper 2001), and they appear to have lost additional telomeric proteins such as Rap1, Rif1 (Kanoh and Ishikawa 2001), and Ku70 (this study) from telomeres. Perhaps the inability of a *taz1*Δ mutation to rescue chromosome circularization in cells without the Rad3/Rad26 and Tel1/Rad32 pathways simply reflects a defect in telomere capping caused by *taz1*Δ. Therefore, it will be interesting to see if mutations in *S. pombe rap1* or *rif1* can rescue chromosome circularization in cells that lack both Rad3/Rad26 and Tel1/Rad32 pathways.

In *S. cerevisiae*, it was observed that telomerase RNA (*tlc1*) deletion hastened the loss of viability of *tel1*Δ *mec1*Δ cells, suggesting that telomerase activity allows cells to partially counteract telomere loss (Chan *et al.* 2001). However, budding yeast *mec1*Δ cells are viable only if the ribonucleotide reductase inhibitor *sml1* is also mutated and an *sml1*Δ mutation itself delays senescence in telomerase and *mec1-21 tel1*Δ mutant cells (Ritchie *et al.* 1999; Longhese *et al.* 2000). Therefore, it is possible that *sml1*Δ helped telomerase to gain limited access to telomeres in *tel1*Δ *mec1*Δ *sml1*Δ cells. Previous studies in *S. cerevisiae* have also found that *tel1*Δ *tlc1*Δ cells lose viability slower than *tlc1*Δ mutants do, suggesting that Tel1 protein may play a role in recruiting both telomerase and exonuclease to telomeres (Ritchie *et al.* 1999).

In our study, we found that *tel1*Δ *rad3*Δ and *tel1*Δ *rad26*Δ cells lost viability much faster than *trt1*Δ cells did, and more importantly we found that this rapid loss of viability was epistatic to a *trt1*Δ mutation. These data suggest that in contrast to *S. cerevisiae*, the presence of functional telomerase does not help to delay senescence in *tel1*Δ *rad3*Δ or *tel1*Δ *rad26*Δ cells. We also found that a *tel1*Δ mutation did not delay senescence caused by a *trt1*Δ mutation, in contrast to *S. cerevisiae*. This was perhaps not a surprise as we found that the telomere maintenance defect in *tel1*Δ and *rad32*Δ cells was revealed only in combination with the loss of the Rad3/Rad26 pathway in our strain backgrounds.

In previous *S. pombe* studies, rapid loss of viability and telomere dysfunction was observed in *pot1*Δ, *pku70*Δ *trt1*Δ, and *taz1*Δ *trt1*Δ cells (Nakamura *et al.* 1998; Baumann and Cech 2000, 2001). Therefore, the loss of the proposed telomere cap (*pot1*Δ) and the simultaneous loss of telomerase and telomere-binding protein (*pku70*Δ *trt1*Δ and *taz1*Δ *trt1*Δ) caused phenotypes similar to *tel1*Δ *rad3*Δ and *tel1*Δ *rad26*Δ cells. Could this

mean that the cells lacking both Rad3/Rad26 and Tel1/Rad32 pathways have defects not only in telomerase recruitment, but also in telomere protection? We believe that this is likely the case since both the senescence rate comparison results and the inability of a *taz1*Δ mutation to rescue chromosome circularization indicate that cells missing both Rad3/Rad26 and Tel1/Rad32 pathways have telomere defects more severe than those of the telomerase mutant.

In this study, we assigned Ku70 to the pathway involving the Rad3/Rad26 and Rad1/Rad9/Hus1/Rad17 functional groups on the basis of our epistasis analysis of steady-state telomere lengths among mutant combinations. However, the rapid senescence phenotype observed in *pku70*Δ *trt1*Δ cannot be easily explained by such a simple assignment, since *rad3*Δ *trt1*Δ and *rad26*Δ *trt1*Δ cells did not lose their viability as rapidly as *pku70*Δ *trt1*Δ cells in most cases. We believe the wide-ranging variability of senescence rates among different clones of *rad3*Δ *trt1*Δ and *rad26*Δ *trt1*Δ is related to the lack of checkpoint function in these cells, since we observed similar wide-ranging senescence rates for *chk1*Δ *trt1*Δ cells. Therefore, *pku70*Δ appears to manifest a synergistic loss of telomere protection in combination with the elimination of telomerase, but such synergistic loss of telomere protection is not apparent in the loss of either the Rad3/Rad26 or the Tel1/Rad32 pathway alone. In contrast, the cells lacking both Rad3/Rad26 and Tel1/Mre11 pathways lose viability rapidly and thus appear to lack protection of telomeres. Therefore, we propose that telomerase, Ku70, and other unidentified factors, which are critical for telomere maintenance and protection, are redundantly recruited to telomeres by the Rad3/Rad26 and Tel1/Rad32 pathways. Therefore, while we did not observe loss of Ku70 binding to telomere in either *rad3*Δ or *tel1*Δ single-mutant cells, we might expect *tel1*Δ *rad3*Δ cells to lose Ku70 binding. Our data also indicate that the rapid senescence observed in *taz1*Δ *trt1*Δ cells might also be caused by the loss of telomerase, Ku70, and other telomere factors from telomeres.

In mammalian cells, Ku70 and Mre11 interact physically, and targeting of Mre11 upon DNA damage to subnuclear foci, which potentially represent sites of DNA repair, is impaired in *ku70* mutant cells (Goedecke *et al.* 1999). Recent studies in *S. cerevisiae* found that the Mre11-Rad50-Xrs2 complex is essential for creation of *de novo* telomeres and loading of the telomere-capping protein Cdc13 to *de novo* telomeres (Diede and Gottschling 2001), while the Mre11-Rad50-Xrs2 was not required for loading of Cdc13 to preexisting telomeres (Tsukamoto *et al.* 2001) or telomere maintenance in the presence of an intact Mec1 pathway (Boulton and Jackson 1998; Nugent *et al.* 1998). Therefore, the Mre11 complex and Ku heterodimer show complex interdependency for their recruitment to sites of damage or telomeres in other organisms. It will be a challenge in the future to sort out how various DNA repair and checkpoint complexes interact to facilitate DNA repair and telomere maintenance processes.

While DNA damage checkpoint proteins were originally identified as proteins required for establishing a cell cycle arrest following DNA damage, recent studies indicate that some of the members of checkpoint proteins are also important for efficient repair of DNA damage (Khanna and Jackson 2001). Our study contributes to the growing evidence that cells also utilize checkpoint sensor and DNA repair proteins to recognize and maintain telomeres. Telomere maintenance is a challenging and complex task, as the telomeres must be recognized as special DNA ends that need to be maintained rather than repaired. As there are many parallels in recognition of damaged DNA and telomeres, understanding how these proteins function at telomeres will also give us a better understanding of how these proteins contribute to recognition and repair of DNA damage.

We thank T. Carr, T. Cech, J. Cooper, T. Enoch, S. Forsburg, and N. Rhind for various *S. pombe* strains and J. Kanoh and F. Ishikawa for a taz1-HA strain and help with ChIP assay. We also thank J. Cooper, V. Géli, and N. Rhind for critical reading of the manuscript. T.M.N. is supported by fellowship DRG-1565 of the Damon Runyon Cancer Research Foundation. B.A.M. was supported in part by a fellowship from the Deutsche Forschungsgesellschaft. This work was funded by National Institutes of Health grants awarded to P.R.

LITERATURE CITED

Ahmed, S., and J. Hodgkin, 2000 MRT-2 checkpoint protein is required for germline immortality and telomere replication in C. elegans. Nature **403:** 159–164.

Alfa, C., P. Fantes, J. Hyams, M. McLoed and E. Warbrick, 1993 *Experiments With Fission Yeast.* Cold Spring Harbor Laboratory Press, Cold Spring Harbor, NY.

al-Khodairy, F., and A. M. Carr, 1992 DNA repair mutants defining G2 checkpoint pathways in Schizosaccharomyces pombe. EMBO J. **11:** 1343–1350.

al-Khodairy, F., E. Fotou, K. S. Sheldrick, D. J. Griffiths, A. R. Lehmann *et al.*, 1994 Identification and characterization of new elements involved in checkpoint and feedback controls in fission yeast. Mol. Biol. Cell **5:** 147–160.

Bähler, J., J. Q. Wu, M. S. Longtine, N. G. Shah, A. McKenzie, III *et al.*, 1998 Heterologous modules for efficient and versatile PCR-based gene targeting in Schizosaccharomyces pombe. Yeast **14:** 943–951.

Bao, S., R. S. Tibbetts, K. M. Brumbaugh, Y. Fang, D. A. Richardson *et al.*, 2001 ATR/ATM-mediated phosphorylation of human Rad17 is required for genotoxic stress responses. Nature **411:** 969–974.

Baumann, P., and T. R. Cech, 2000 Protection of telomeres by the Ku protein in fission yeast. Mol. Biol. Cell **11:** 3265–3275.

Baumann, P., and T. R. Cech, 2001 Pot1, the putative telomere end-binding protein in fission yeast and humans. Science **292:** 1171–1175.

Bentley, N. J., D. A. Holtzman, G. Flaggs, K. S. Keegan, A. DeMaggio *et al.*, 1996 The Schizosaccharomyces pombe rad3 checkpoint gene. EMBO J. **15:** 6641–6651.

Blackburn, E. H., 2001 Switching and signaling at the telomere. Cell **106:** 661–673.

Boddy, M. N., B. Furnari, O. Mondesert and P. Russell, 1998 Replication checkpoint enforced by kinases Cds1 and Chk1. Science **280:** 909–912.

Boulton, S. J., and S. P. Jackson, 1998 Components of the Ku-

dependent non-homologous end-joining pathway are involved in telomeric length maintenance and telomeric silencing. EMBO J. **17:** 1819–1828.

Brush, G. S., and T. J. Kelly, 2000 Phosphorylation of the replication protein A large subunit in the Saccharomyces cerevisiae checkpoint response. Nucleic Acids Res. **28:** 3725–3732.

Cai, R. L., Y. Yan-Neale, M. A. Cueto, H. Xu and D. Cohen, 2000 HDAC1, a histone deacetylase, forms a complex with Hus1 and Rad9, two G2/M checkpoint Rad proteins. J. Biol. Chem. **275:** 27909–27916.

Caspari, T., and A. M. Carr, 1999 DNA structure checkpoint pathways in Schizosaccharomyces pombe. Biochimie **81:** 173–181.

Caspari, T., M. Dahlen, G. Kanter-Smoler, H. D. Lindsay, K. Hofmann *et al.*, 2000 Characterization of Schizosaccharomyces pombe Hus1: a PCNA-related protein that associates with Rad1 and Rad9. Mol. Cell. Biol. **20:** 1254–1262.

Chan, S. W., J. Chang, J. Prescott and E. H. Blackburn, 2001 Altering telomere structure allows telomerase to act in yeast lacking ATM kinases. Curr. Biol. **11:** 1240–1250.

Cooper, J. P., E. R. Nimmo, R. C. Allshire and T. R. Cech, 1997 Regulation of telomere length and function by a Myb-domain protein in fission yeast. Nature **385:** 744–747.

Corda, Y., V. Schramke, M. P. Longhese, T. Smokvina, V. Paciotti *et al.*, 1999 Interaction between Set1p and checkpoint protein Mec3p in DNA repair and telomere functions. Nat. Genet. **21:** 204–208.

Craven, R. J., and T. D. Petes, 1999 Dependence of the regulation of telomere length on the type of subtelomeric repeat in the yeast *Saccharomyces cerevisiae*. Genetics **152:** 1531–1541.

d'Adda di Fagagna, F., M. P. Hande, W. M. Tong, D. Roth, P. M. Lansdorp *et al.*, 2001 Effects of DNA nonhomologous end-joining factors on telomere length and chromosomal stability in mammalian cells. Curr. Biol. **11:** 1192–1196.

D'Amours, D., and S. P. Jackson, 2001 The yeast Xrs2 complex functions in S phase checkpoint regulation. Genes Dev. **15:** 2238–2249.

Dahlén, M., T. Olsson, G. Kanter-Smoler, A. Ramne and P. Sunnerhagen, 1998 Regulation of telomere length by checkpoint genes in Schizosaccharomyces pombe. Mol. Biol. Cell **9:** 611–621.

Diede, S. J., and D. E. Gottschling, 2001 Exonuclease activity is required for sequence addition and Cdc13p loading at a de novo telomere. Curr. Biol. **11:** 1336–1340.

Edwards, R. J., N. J. Bentley and A. M. Carr, 1999 A Rad3-Rad26 complex responds to DNA damage independently of other checkpoint proteins. Nat. Cell Biol. **1:** 393–398.

Ferreira, M. G., and J. P. Cooper, 2001 The fission yeast Taz1 protein protects chromosomes from Ku-dependent end-to-end fusions. Mol. Cell **7:** 55–63.

Gatei, M., D. Young, K. M. Cerosaletti, A. Desai-Mehta, K. Spring *et al.*, 2000 ATM-dependent phosphorylation of nibrin in response to radiation exposure. Nat. Genet. **25:** 115–119.

Goedecke, W., M. Eijpe, H. H. Offenberg, M. van Aalderen and C. Heyting, 1999 Mre11 and Ku70 interact in somatic cells, but are differentially expressed in early meiosis. Nat. Genet. **23:** 194–198.

Grandin, N., C. Damon and M. Charbonneau, 2001 Cdc13 prevents telomere uncapping and Rad50-dependent homologous recombination. EMBO J. **20:** 6127–6139.

Gravel, S., M. Larrivee, P. Labrecque and R. J. Wellinger, 1998 Yeast Ku as a regulator of chromosomal DNA end structure. Science **280:** 741–744.

Griffith, J. D., L. A. Lindsey-Boltz and A. Sancar, 2002 Structures of the human rad17-replication factor C and checkpoint rad 9-1-1 complexes visualized by glycerol spray/low voltage microscopy. J. Biol. Chem. **277:** 15233–15236.

Griffiths, D. J., N. C. Barbet, S. McCready, A. R. Lehmann and A. M. Carr, 1995 Fission yeast rad17: a homologue of budding yeast RAD24 that shares regions of sequence similarity with DNA polymerase accessory proteins. EMBO J. **14:** 5812–5823.

Grimm, C., J. Kohli, J. Murray and K. Maundrell, 1988 Genetic engineering of Schizosaccharomyces pombe: a system for gene disruption and replacement using the ura4 gene as a selectable marker. Mol. Gen. Genet. **215:** 81–86.

Haering, C. H., T. M. Nakamura, P. Baumann and T. R. Cech, 2000 Analysis of telomerase catalytic subunit mutants in vivo and in vitro in Schizosaccharomyces pombe. Proc. Natl. Acad. Sci. USA **97:** 6367–6372.

Hardy, C. F., L. Sussel and D. Shore, 1992 A RAP1-interacting protein involved in transcriptional silencing and telomere length regulation. Genes Dev. **6:** 801–814.

Hartsuiker, E., E. Vaessen, A. M. Carr and J. Kohli, 2001 Fission yeast Rad50 stimulates sister chromatid recombination and links cohesion with repair. EMBO J. **20:** 6660–6671.

Hsu, H. L., D. Gilley, E. H. Blackburn and D. J. Chen, 1999 Ku is associated with the telomere in mammals. Proc. Natl. Acad. Sci. USA **96:** 12454–12458.

Hsu, H. L., D. Gilley, S. A. Galande, M. P. Hande, B. Allen *et al.*, 2000 Ku acts in a unique way at the mammalian telomere to prevent end joining. Genes Dev. **14:** 2807–2812.

Kai, M., H. Tanaka and T. S. Wang, 2001 Fission yeast Rad17 associates with chromatin in response to aberrant genomic structures. Mol. Cell. Biol. **21:** 3289–3301.

Kanoh, J., and F. Ishikawa, 2001 spRap1 and spRif1, recruited to telomeres by Taz1, are essential for telomere function in fission yeast. Curr. Biol. **11:** 1624–1630.

Kaur, R., C. F. Kostrub and T. Enoch, 2001 Structure-function analysis of fission yeast hus1-rad1-rad9 checkpoint complex. Mol. Biol. Cell **12:** 3744–3758.

Khanna, K. K., and S. P. Jackson, 2001 DNA double-strand breaks: signaling, repair and the cancer connection. Nat. Genet. **27:** 247–254.

Kishi, S., X. Z. Zhou, Y. Ziv, C. Khoo, D. E. Hill *et al.*, 2001 Telomeric protein Pin2/TRF1 as an important ATM target in response to double strand DNA breaks. J. Biol. Chem. **276:** 29282–29291.

Kondo, T., T. Wakayama, T. Naiki, K. Matsumoto and K. Sugimoto, 2001 Recruitment of Mec1 and Ddc1 checkpoint proteins to double-strand breaks through distinct mechanisms. Science **294:** 867–870.

Kostrub, C. F., F. al-Khodairy, H. Ghazizadeh, A. M. Carr and T. Enoch, 1997 Molecular analysis of hus1+, a fission yeast gene required for S-M and DNA damage checkpoints. Mol. Gen. Genet. **254:** 389–399.

Krawchuk, M. D., and W. P. Wahls, 1999 High-efficiency gene targeting in Schizosaccharomyces pombe using a modular, PCR-based approach with long tracts of flanking homology. Yeast **15:** 1419–1427.

Lieberman, H. B., K. M. Hopkins, M. Laverty and H. M. Chu, 1992 Molecular cloning and analysis of Schizosaccharomyces pombe rad9, a gene involved in DNA repair and mutagenesis. Mol. Gen. Genet. **232:** 367–376.

Lim, D. S., S. T. Kim, B. Xu, R. S. Maser, J. Lin *et al.*, 2000 ATM phosphorylates p95/nbs1 in an S-phase checkpoint pathway. Nature **404:** 613–617.

Lombard, D. B., and L. Guarente, 2000 Nijmegen breakage syndrome disease protein and MRE11 at PML nuclear bodies and meiotic telomeres. Cancer Res. **60:** 2331–2334.

Longhese, M. P., V. Paciotti, H. Neecke and G. Lucchini, 2000 Checkpoint proteins influence telomeric silencing and length maintenance in budding yeast. Genetics **155:** 1577–1591.

Manolis, K. G., E. R. Nimmo, E. Hartsuiker, A. M. Carr, P. A. Jeggo *et al.*, 2001 Novel functional requirements for non-homologous DNA end joining in Schizosaccharomyces pombe. EMBO J. **20:** 210–221.

Matsuura, A., T. Naito and F. Ishikawa, 1999 Genetic control of telomere integrity in *Schizosaccharomyces pombe*: rad3(+) and tel1(+) are parts of two regulatory networks independent of the downstream protein kinases chk1(+) and cds1(+). Genetics **152:** 1501–1512.

Melo, J. A., J. Cohen and D. P. Toczyski, 2001 Two checkpoint complexes are independently recruited to sites of DNA damage in vivo. Genes Dev. **15:** 2809–2821.

Moser, B. A., J. M. Brondello, B. Baber-Furnari and P. Russell, 2000 Mechanism of caffeine-induced checkpoint override in fission yeast. Mol. Cell. Biol. **20:** 4288–4294.

Murray, J. M., A. M. Carr, A. R. Lehmann and F. Z. Watts, 1991 Cloning and characterisation of the rad9 DNA repair gene from Schizosaccharomyces pombe. Nucleic Acids Res. **19:** 3525–3531.

Naito, T., A. Matsuura and F. Ishikawa, 1998 Circular chromosome formation in a fission yeast mutant defective in two ATM homologues. Nat. Genet. **20:** 203–206.

Nakamura, T. M., G. B. Morin, K. B. Chapman, S. L. Weinrich,

W. H. Andrews *et al.*, 1997 Telomerase catalytic subunit homologs from fission yeast and human. Science **277:** 955–959.

Nakamura, T. M., J. P. Cooper and T. R. Cech, 1998 Two modes of survival of fission yeast without telomerase. Science **282:** 493–496.

Nugent, C. I., G. Bosco, L. O. Ross, S. K. Evans, A. P. Salinger *et al.*, 1998 Telomere maintenance is dependent on activities required for end repair of double-strand breaks. Curr. Biol. **8:** 657–660.

Oakley, G. G., L. I. Loberg, J. Yao, M. A. Risinger, R. L. Yunker *et al.*, 2001 UV-induced hyperphosphorylation of replication protein a depends on DNA replication and expression of ATM protein. Mol. Biol. Cell **12:** 1199–1213.

Orlando, V., and R. Paro, 1993 Mapping polycomb-repressed domains in the bithorax complex using in vivo formaldehyde cross-linked chromatin. Cell **75:** 1187–1198.

Paciotti, V., G. Lucchini, P. Plevani and M. P. Longhese, 1998 Mec1p is essential for phosphorylation of the yeast DNA damage checkpoint protein Ddc1p, which physically interacts with Mec3p. EMBO J. **17:** 4199–4209.

Post, S., Y. C. Weng, K. Cimprich, L. B. Chen, Y. Xu *et al.*, 2001 Phosphorylation of serines 635 and 645 of human Rad17 is cell cycle regulated and is required for G(1)/S checkpoint activation in response to DNA damage. Proc. Natl. Acad. Sci. USA **98:** 13102–13107.

Ray, A., and K. W. Runge, 1999 Varying the number of telomere-bound proteins does not alter telomere length in tel1Delta cells. Proc. Natl. Acad. Sci. USA **96:** 15044–15049.

Rhind, N., and P. Russell, 1998 Mitotic DNA damage and replication checkpoints in yeast. Curr. Opin. Cell Biol. **10:** 749–758.

Rigaut, G., A. Shevchenko, B. Rutz, M. Wilm, M. Mann *et al.*, 1999 A generic protein purification method for protein complex characterization and proteome exploration. Nat. Biotechnol. **17:** 1030–1032.

Ritchie, K. B., and T. D. Petes, 2000 The Mre11p/Rad50p/Xrs2p complex and the Tel1p function in a single pathway for telomere maintenance in yeast. Genetics **155:** 475–479.

Ritchie, K. B., J. C. Mallory and T. D. Petes, 1999 Interactions of TLC1 (which encodes the RNA subunit of telomerase), TEL1, and MEC1 in regulating telomere length in the yeast Saccharomyces cerevisiae. Mol. Cell. Biol. **19:** 6065–6075.

Rouse, J., and S. P. Jackson, 2002 Lcd1p recruits Mec1p to DNA lesions in vitro and in vivo. Mol. Cell **9:** 857–869.

Saka, Y., F. Esashi, T. Matsusaka, S. Mochida and M. Yanagida, 1997 Damage and replication checkpoint control in fission yeast is ensured by interactions of Crb2, a protein with BRCT motif, with Cut5 and Chk1. Genes Dev. **11:** 3387–3400.

Song, K., D. Jung, Y. Jung, S. G. Lee and I. Lee, 2000 Interaction of human Ku70 with TRF2. FEBS Lett. **481:** 81–85.

Strahl-Bolsinger, S., A. Hecht, K. Luo and M. Grunstein, 1997 SIR2 and SIR4 interactions differ in core and extended telomeric heterochromatin in yeast. Genes Dev. **11:** 83–93.

Sugawara, N. F., 1988 DNA sequences at the telomeres of the fission yeast *S. pombe*. Ph.D. Thesis, Harvard University, Cambridge, MA.

Sunnerhagen, P., B. L. Seaton, A. Nasim and S. Subramani, 1990 Cloning and analysis of a gene involved in DNA repair and recombination, the rad1 gene of Schizosaccharomyces pombe. Mol. Cell. Biol. **10:** 3750–3760.

Tavassoli, M., M. Shayeghi, A. Nasim and F. Z. Watts, 1995 Cloning and characterisation of the Schizosaccharomyces pombe rad32 gene: a gene required for repair of double strand breaks and recombination. Nucleic Acids Res. **23:** 383–388.

Tsukamoto, Y., A. K. Taggart and V. A. Zakian, 2001 The role of the Mre11-Rad50-Xrs2 complex in telomerase-mediated lengthening of Saccharomyces cerevisiae telomeres. Curr. Biol. **11:** 1328–1335.

Usui, T., H. Ogawa and J. H. Petrini, 2001 A DNA damage response pathway controlled by Tel1 and the Mre11 complex. Mol. Cell **7:** 1255–1266.

Venclovas, C., and M. P. Thelen, 2000 Structure-based predictions of Rad1, Rad9, Hus1 and Rad17 participation in sliding clamp and clamp-loading complexes. Nucleic Acids Res. **28:** 2481–2493.

Vialard, J. E., C. S. Gilbert, C. M. Green and N. F. Lowndes, 1998 The budding yeast Rad9 checkpoint protein is subjected to Mec1/Tel1-dependent hyperphosphorylation and interacts with Rad53 after DNA damage. EMBO J. **17:** 5679–5688.

Wach, A., A. Brachat, R. Pohlmann and P. Philippsen, 1994 New heterologous modules for classical or PCR-based gene disruptions in Saccharomyces cerevisiae. Yeast **10:** 1793–1808.

Wang, H., J. Guan, A. R. Perrault, Y. Wang and G. Iliakis, 2001 Replication protein A2 phosphorylation after DNA damage by the coordinated action of ataxia telangiectasia-mutated and DNA-dependent protein kinase. Cancer Res. **61:** 8554–8563.

Wilson, S., M. Tavassoli and F. Z. Watts, 1998 Schizosaccharomyces pombe rad32 protein: a phosphoprotein with an essential phosphoesterase motif required for repair of DNA double strand breaks. Nucleic Acids Res. **26:** 5261–5269.

Wilson, S., N. Warr, D. L. Taylor and F. Z. Watts, 1999 The role of Schizosaccharomyces pombe Rad32, the Mre11 homologue, and other DNA damage response proteins in non-homologous end joining and telomere length maintenance. Nucleic Acids Res. **27:** 2655–2661.

Wolkow, T. D., and T. Enoch, 2002 Fission yeast rad26 is a regulatory subunit of the rad3 checkpoint kinase. Mol. Biol. Cell **13:** 480–492.

Wotton, D., and D. Shore, 1997 A novel Rap1p-interacting factor, Rif2p, cooperates with Rif1p to regulate telomere length in Saccharomyces cerevisiae. Genes Dev. **11:** 748–760.

Zhu, X. D., B. Kuster, M. Mann, J. H. Petrini and T. Lange, 2000 Cell-cycle-regulated association of RAD50/MRE11/NBS1 with TRF2 and human telomeres. Nat. Genet. **25:** 347–352.

Communicating editor: G. Smith

TABLE S1
***S. pombe* strains used in this study**

Name in Figures	Strain	Genotype*
wt	TMN2665	*h⁻ ade6-M210*
wt	TMN2663	*h⁺ ade6-M216*
rad1Δ	TMN2929	*h⁻ rad1::ura4⁺ ade6-M216*
rad9Δ	TMN2931	*h⁻ rad9::ura4⁺ ade6-M216*
hus1Δ	TMN2933	*h⁻ hus1::LEU2 ade6-M216*
rad17Δ	TMN2935	*h⁻ rad17::ura4⁺ ade6-M216*
rad3Δ	TMN2937	*h⁻ rad3::ura4⁺ ade6-M216*
rad26Δ	TMN2939	*h⁻ rad26::ura4⁺ ade6-M216*
crb2Δ	TMN2941	*h⁻ crb2::ura4⁺ ade6-M216*
chk1Δ	TMN2943	*h⁻ chk1::ura4⁺ ade6-M216*
cds1Δ	TMN2945	*h⁻ cds1::ura4⁺ ade6-M216*
chk1Δ cds1Δ	BF2115 (1)	*h⁺ chk1::ura4⁺ cds1::ura4⁺*
rad1Δ hus1Δ	TMN2949	*h⁻ rad1::ura4⁺ hus1::LEU2 ade6-M216*
rad9Δ hus1Δ	TMN2951	*h⁻ rad9::ura4⁺ hus1::LEU2 ade6-M216*
rad17Δ hus1Δ	TMN2953	*h⁻ rad17::ura4⁺ hus1::LEU2 ade6-M216*
rad3Δ rad26Δ	TMN2955	*h⁻ rad3-D2::LEU2 rad26::ura4⁺ ade6-M216*
rad3Δ rad1Δ	TMN2957	*h⁻ rad3-D2::LEU2 rad1::ura4⁺ ade6-M216*
rad3Δ rad9Δ	TMN2959	*h⁻ rad3-D2::LEU2 rad9::ura4⁺ ade6-M210*
rad3Δ hus1Δ	TMN2961	*h⁻ rad3::ura4⁺ hus1::LEU2 ade6-M216*
rad3Δ rad17Δ	TMN2963	*h⁻ rad3-D2::LEU2 rad17::ura4⁺ ade6-M216*
rad26Δ hus1Δ	TMN2965	*h⁻ rad26::ura4⁺ hus1::LEU2 ade6-M216*
tel1Δ	TMN2967	*h⁻ tel1-D1::kanMX4 ade6-M210*
tel1Δ rad1Δ	TMN2970	*h⁻ tel1-D1::kanMX4 rad1::ura4⁺ ade6-M210*
tel1Δ rad9Δ	TMN2972	*h⁻ tel1-D1::kanMX4 rad9::ura4⁺ ade6-M210*
tel1Δ hus1Δ	TMN2974	*h⁻ tel1-D1::kanMX4 hus1::LEU2 ade6-M210*
tel1Δ rad17Δ	TMN2976	*h⁻ tel1-D1::kanMX4 rad17::ura4⁺ ade6-M210*
tel1Δ rad3Δ	TMN2978	*h? tel1-D1::kanMX4 rad3::ura4⁺ ade6-M210*
tel1Δ rad26Δ	TMN2979	*h? tel1-D1::kanMX4 rad26::ura4⁺ ade6-M216*
tel1Δ crb2Δ	TMN2980	*h⁻ tel1-D1::kanMX4 crb2::ura4⁺ ade6-M210*
tel1Δ chk1Δ	TMN2982	*h⁻ tel1-D1::kanMX4 chk1::ura4⁺ ade6-M210*
tel1Δ cds1Δ	TMN2984	*h⁻ tel1-D1::kanMX4 cds1::ura4⁺ ade6-M210*
tel1Δ chk1Δ cds1Δ	TMN2986	*h⁻ tel1-D1::kanMX4 chk1::ura4⁺ cds1::ura4⁺ ade6-M210*
rad32Δ	TMN2799	*h⁻ rad32-D1::kanMX4 ade6-M210*
rad32Δ	TMN2800	*h⁺ rad32-D1::kanMX4 ade6-M210*
rad32Δ tel1Δ	TMN2988	*h⁻ rad32-D1::kanMX4 tel1-D1::kanMX4 ade6-M216*
rad32Δ rad1Δ	TMN2990	*h⁺ rad32-D1::kanMX4 rad1::ura4⁺ ade6-M216*
rad32Δ rad9Δ	TMN2991	*h⁺ rad32-D1::kanMX4 rad9::ura4⁺ ade6-M216*
rad32Δ hus1Δ	TMN2992	*h⁺ rad32-D1::kanMX4 hus1::LEU2 ade6-M216*
rad32Δ rad17Δ	TMN2993	*h⁺ rad32-D1::kanMX4 rad17::ura4⁺ ade6-M216*
rad32Δ rad3Δ	TMN2994	*h? rad32-D1::kanMX4 rad3::ura4⁺ ade6-?*
rad32Δ rad26Δ	TMN2995	*h? rad32-D1::kanMX4 rad26::ura4⁺ ade6-?*
rad32Δ crb2Δ	TMN2996	*h⁺ rad32-D1::kanMX4 crb2::ura4⁺ ade6-M216*
rad32Δ chk11Δ	TMN2997	*h⁺ rad32-D1::kanMX4 chk1::ura4⁺ ade6-M216*
rad32Δ cds1Δ	TMN2998	*h⁺ rad32-D1::kanMX4 cds1::ura4⁺ ade6-M216*

rad32Δ chk1Δ cds1Δ	TMN2999 [1]	*h⁺ rad32-D1::kanMX4 chk1::ura4⁺ cds1::ura4⁺*
pku70Δ	TMN3000	*h⁻ pku70-D1::kanMX4 ade6-M210*
pku70Δ rad1Δ	TMN3002	*h⁻ pku70-D1::kanMX4 rad1::ura4⁺ ade6-M216*
pku70Δ rad9Δ	TMN3004	*h⁻ pku70-D1::kanMX4 rad9::ura4⁺ ade6-M216*
pku70Δ hus1Δ	TMN3006	*h⁻ pku70-D1::kanMX4 hus1::LEU2 ade6-M216*
pku70Δ rad17Δ	TMN3008	*h⁻ pku70-D1::kanMX4 rad17::ura4⁺ ade6-M216*
pku70Δ rad3Δ	TMN3010	*h⁻ pku70-D1::kanMX4 rad3::ura4⁺ ade6-M216*
pku70Δ rad26Δ	TMN3012	*h⁻ pku70-D1::kanMX4 rad26::ura4⁺ ade6-M216*
pku70Δ crb2Δ	TMN3014	*h⁻ pku70-D1::kanMX4 crb2::ura4⁺ ade6-M216*
pku70Δ chk1Δ	TMN3016	*h⁻ pku70-D1::kanMX4 chk1::ura4⁺ ade6-M216*
pku70Δ cds1Δ	TMN3018	*h⁻ pku70-D1::kanMX4 cds1::ura4⁺ ade6-M216*
pku70Δ chk1Δ cds1Δ	TMN3020 [1]	*h⁺ pku70-D1::kanMX4 chk1::ura4⁺ cds1::ura4⁺*
pku70Δ tel1Δ	TMN3021	*h⁻ pku70-D1::kanMX4 tel1-D1::kanMX4 ade6-M210*
pku70Δ rad32Δ	TMN3023	*h⁻ pku70-D1::kanMX4 rad32-D1::kanMX4 ade6-M210*
pku70Δ tel1Δ rad1Δ	TMN3025	*h⁺ pku70-D1::kanMX4 tel1-D1::kanMX4 rad1::ura4⁺ ade6-M210*
pku70Δ tel1Δ rad9Δ	TMN3026	*h⁺ pku70-D1::kanMX4 tel1-D1::kanMX4 rad9::ura4⁺ ade6-M210*
pku70Δ tel1Δ hus1Δ	TMN3027	*h⁻ pku70-D1::kanMX4 tel1-D1::kanMX4 hus1::LEU2 ade6-M210*
pku70Δ tel1Δ rad17Δ	TMN3028	*h⁻ pku70-D1::kanMX4 tel1-D1::kanMX4 rad17::ura4⁺ ade6-M210*
pku70Δ tel1Δ rad3Δ	TMN3029	*h⁻ pku70-D1::kanMX4 tel1-D1::kanMX4 rad3::ura4⁺ ade6-M216*
taz1Δ	TMN2666	*h⁻ taz1::ura4⁺ ade6-M210*
taz1Δ rad1Δ	TMN3030	*h⁻ taz1-D3::LEU2 rad1::ura4⁺ ade6-M216*
taz1Δ rad9Δ	TMN3031	*h⁻ taz1-D3::LEU2 rad9::ura4⁺ ade6-M216*
taz1Δ hus1Δ	TMN3032	*h⁻ taz1::ura4⁺ hus1::LEU2 ade6-M216*
taz1Δ rad17Δ	TMN3033	*h⁻ taz1-D3::LEU2 rad17::ura4⁺ ade6-M216*
taz1Δ rad3Δ	TMN3034	*h⁻ taz1-D3::LEU2 rad3::ura4⁺ ade6-M216*
taz1Δ rad26Δ	TMN3035	*h⁻ taz1-D3::LEU2 rad26::ura4⁺ ade6-M216*
taz1Δ crb2Δ	TMN3036	*h⁻ taz1-D3::LEU2 crb2::ura4⁺ ade6-M216*
taz1Δ chk1Δ	TMN3037	*h⁻ taz1-D3::LEU2 chk1::ura4⁺ ade6-M216*
taz1Δ cds1Δ	TMN3038	*h⁻ taz1-D3::LEU2 cds1::ura4⁺ ade6-M216*
taz1Δ chk1Δ cds1Δ	TMN3039 [1]	*h⁺ taz1-D4::kanMX4 chk1::ura4⁺ cds1::ura4⁺*
taz1Δ tel1Δ	TMN3040	*h⁺ taz1::ura4⁺ tel1-D1::kanMX4 ade6-M210*
taz1Δ rad32Δ	TMN3041	*h⁻ taz1::ura4⁺ rad32-D1::kanMX4 ade6-M210*
taz1Δ pku70Δ	TMN3042	*h⁻ taz1::ura4⁺ pku70-D1::kanMX4 ade6-M210*
taz1Δ tel1Δ rad3Δ	TMN3043	*h⁻ taz1-D3::LEU2 tel1-D1::kanMX4 rad3::ura4⁺ ade6-M216*
taz1Δ tel1Δ rad26Δ	TMN3044	*h⁻ taz1-D3::LEU2 tel1-D1::kanMX4 rad26::ura4⁺ ade6-M216*
taz1Δ rad32Δ rad3Δ	TMN3045	*h⁻ taz1-D3::LEU2 rad32-D1::kanMX4 rad3::ura4⁺ ade6-M216*
taz1Δ rad32Δ rad26Δ	TMN3046	*h⁻ taz1-D3::LEU2 rad32-D1::kanMX4 rad26::ura4⁺ ade6-M216*
trt1Δ	TMN2669	*h⁻ trt1-D2::his3⁺ ade6-M210*
taz1Δ trt1Δ	TMN2672	*h⁻ taz1::ura4⁺ trt1-D2::his⁺ ade6-M210*
	TMN3047 [2]	*h⁺/h⁻ trt1-D2::his3⁺/trt1⁺*
	TMN3048 [2]	*h⁺/h⁻ trt1-D2::his3⁺/trt1⁺ rad3::ura4⁺/rad3⁺*
	TMN3049 [2]	*h⁺/h⁻ trt1-D2::his3⁺/trt1⁺ rad26::ura4⁺/rad26⁺*
	TMN3052 [2]	*h⁺/h⁻ trt1-D2::his3⁺/trt1⁺ tel1-D1::kanMX4/tel1⁺ rad3::ura4⁺/rad3⁺*
	TMN3053 [2]	*h⁺/h⁻ trt1-D2::his3⁺/trt1⁺ tel1-D1::kanMX4/tel1⁺ rad26::ura4⁺/rad26⁺*
rad32-TAP	TMN2842	*h⁻ rad32⁺::TAP-kanMX6 ade6-M210*
rad3Δ rad32-TAP	TMN3058	*h⁻ rad3::ura4⁺ rad32⁺::TAP-kanMX6 ade6-M210*
tel1Δ rad32-TAP	TMN3064	*h⁻ tel1-D2::LEU2 rad32⁺::TAP-kanMX6 ade6-M210*
tel1Δ rad3Δ rad32-TAP	TMN3065	*h⁻ tel1-D2::LEU2 rad3::ura4⁺ rad32⁺::TAP-kanMX6 ade6-M210*

rad32-myc	TMN2843	*h⁻ rad32⁺::13myc-kanMX6 ade6-M210*
wt	PR109 [(1)]	*h⁻*
nmt-HA-rad3	BF2039 [(3)]	*h- rad3::nmt-3HA-rad3⁺-ura4⁺*
HA-rad3	BF2453 [(1)]	*h⁻ rad3::3HA-rad3⁺*
rad1-myc	BM3068 [(1)]	*h⁺ rad1⁺::13myc-kanMX6*
rad9-myc	BM3069 [(1)]	*h⁻ rad9⁺::13myc-kanMX6*
hus1-myc	BM3070 [(1)]	*h⁻ hus1⁺::13myc-kanMX6*
rad17-myc	BM3071 [(1)]	*h⁺ rad17⁺::13myc-kanMX6*
taz1-HA	BM3072 [(1)]	*h⁺ taz1⁺::3HA-ura4⁺*
pku70-myc	BM3073	*h⁻ pku70⁺::13myc-kanMX6 ade6-M210*
pku70-HA	BM3074	*h⁻ pku70⁺::3HA-kanMX6 ade6-M210*
rad17Δ pku70-HA	BM3075	*h⁻ rad17::ura4⁺ pku70⁺::3HA-kanMX6 ade6-M210*
rad3Δ pku70-HA	BM3076	*h⁻ rad3::ura4⁺ pku70⁺::3HA-kanMX6 ade6-M210*
tel1Δ pku70-HA	BM3077	*h⁻ tel1-D2::LEU2 pku70⁺::3HA-kanMX6 ade6-M210*
taz1Δ pku70-HA	BM3078	*h⁻ taz1::ura4⁺ pku70⁺::3HA-kanMX6 ade6-M210*

[*]Most strains are also *leu1-32 ura4-D18 his3-D1*, except for strains denoted with [(1)] (*leu1-32 ura4-D18*), [(2)] (*leu1-32/leu1-32 ura4-D18/ura4-D18 ade6-M210/ade6-M216 his3-D1/his3-D1*) or [(3)] (*ura4-294*).

TABLE S2

DNA Oligonucleotide Primers Used in Strain Construction

Name	Sequence (5' to 3')
taz1-LEUT	TTG TTC TAA GGG ATT ATG ATA ATT TTA TAA TTG TTT AGT GAA ATT CGT AAT TCA ACC TCT TTC ACC ATA CAA TCG AGG GCA GTT GAG AAC TTC TAG TAT ATC [1]
taz1-LEUB	CAC GAT TAA CAA AAC TAT CCG AGT CTT GTC AAT ATT ATT CAT TAA AAA AGC AAT CAT GAA CAA ACT CTA TCC GGA GAC GAA AAA CGT CGT AAG GCC GTT TCT [1]
taz1-MX4T	TTG TTC TAA GGG ATT ATG ATA ATT TTA TAA TTG TTT AGT GAA ATT CGT AAT TCA ACC TCT TTC ACC ATA CAA TCG AGG GCA GTT GGT TAA TTA AGG CGC GCC AGA [2]
taz1-MX4B	CAC GAT TAA CAA AAC TAT CCG AGT CTT GTC AAT ATT ATT CAT TAA AAA AGC AAT CAT GAA CAA ACT CTA TCC GGA GAC GAA AAT CAT CGA TGA ATT CGA GCT CG [2]
tazKO-LU	CTC TAA TCA AAT TCA GGA ACT AGA A
tazKO-RB	CCA ATA AAG GAT GAT TAA GGC CGT G
rad32-KO1	ATT ATT CTA AAG CTG TAA AAG GTG TCG CGT CTT CGT GAA GCA GTC ATC TCA TAT ATG GAG TTT TAT TTA CTG CAA TTG CAG GTT AAT TAA GGC GCG CCA GA [2]
rad32-KO2	CCT GAC CAG ATT AGA ACC TAC AAC AAT GGG CTT AAC ATT ACA GTA TCC AAA TAT AGG TAC ACT TAA ACA AAA ATT TGA TAA GTC ATC GAT GAA TTC GAG CTC G [2]
pku70-KO1	GAC ATT TAA GAT ACT AAT GAA ATA GTT ATT TCA TTC GTG TGC TTT AGC CGT TAT CAT CGG ACG GTT TAC ATA AAA TAT CAG CGG TTA ATT AAG GCG CGC CAG A [2]
pku70-KO2	CCT GAT TCC ATT ATT GTT TCA TAA ACA TGA TGC TGA TAT TTA ATC CTT TAA TAT TTT CTT GTT TAT AAT TTT TTG ACA TAG TCA TCG ATG AAT TCG AGC TCG [2]
rad3-LEUT	TCA AGA CTT TGA ACG CGC GTG TTG CGT TTT AAA AAG GCC TTT TTT TGA ATT GAA TCA ATG GTT TGA TAT AGT GAG GAG AAC TTC TAG TAT ATC CAC ATA C [1]
rad3-LEUB	CTA GAA ATA AGC AGC CCA ACC AAT GTA CAT TTC TAC CAG GTT TTT TGG GTT GAC AGC AGA TTT GAT CAA TTC TAC GTC GTA AGG CCG TTT CTG ACA GAG T [1]
tel1-T1	GAT CGA TCC TCG AGT ACG TAC AAT TTT CAG GTT CCA ATA GTA TGA GCT G [4]
tel1-B2	GAG CTA TAC TTA AAG TAA GAC AGA AAT TAT CAA GTA C
tel1-T3	GAT CGC TCT AGA CTG CTC TTG GGA AGC TTT GGA AAT TTG ACG [5]
tel1-B4	GCT TCA TTT AGC GAC GCT GTT TCG TTT ATC
tel1-LEUT	ATG ACT TCT CTA AAT GAC ATC GTT AAT AAG TTG TCT TCA TCA AAA ATC AAA ACA CGA TCA GAT GCT CTA CAA GAG GAG AAC TTC TAG TAT ATC CAC ATA C [1]
tel1-LEUB	TTA ACT ATA TCG CTC ATT GAA AGG CAG ACC ATC CAC AAA ACA TAA GTG CGA GAT ATG AGG GAT CTT GAG CAA TAC GTC GTA AGG CCG TTT CTG ACA GAG T [1]
rad32-tagT	TCT ACG CTT CTA TTT TAC GAC CCA TCC AGC ACC ACA GAA GCG CAG TAC TTG GAT AAC GAG GAT GAC GAA ATT TTA GAT GAT CGG ATC CCC GGG TTA ATT AA [3]
rad32-tagB	ATC ATT TAA TAA CTC TAT TAC TAA ATT AGT TGT ATT TTG GCA GCG ATC CAC GAA CAT CAG GTA AAG AAG CCT GAC CAG GCG GCG TTA GTA TCG AAT CGA C [3]
BAM102	CTC AGG GAT CGT GGA CTT AGA GTG AGC GGT AAA AAG GCA GAT TTA TTA GAC AAT CTA ACG AAC TAT GTC AAA AAA TTA CGG ATC CCC GGG TTA ATT AA [3]
BAM103	CGC TTT AAT AAA ATA ATT TGA TCG TTT TAT AAA CAA GAA ATT TTA TCC TGA TTC CAT TAT TGT TTC ATA AAC ATG ATG CTG TCA TCG ATG AAT TCG AGC TCG [3]
BAM84	GAT GTG AAC GAT GAT GCC GAA TTT GGA CCA ACG CAA GCT GAA CAA AGT TAT CAT GGC ATT TTC TCT CAG GAA GAC CGG ATC CCC GGG TTA ATT AA [3]

BAM85	GGC CGT GGA TTG GAA TTT AAT TAA TTG GGT TAC ATT ATT CAC TAT CTT ATT GAT TTA TTA GAA CTA CTA TGT AAC GTA TCG GAA TTC GAG CTC GTT TAA AC [3]
BAM88	GTA CTT TAT GTT TAT ATA ACA GAT CCA GAA GAT GAA CAT ACG GCT GTT TTA ACA TAC TAC ATT AGT ACC TAT GTG GAC CGG ATC CCC GGG TTA ATT AA [3]
BAM89	GGA AGA GAG AGA AAA TAA GTA TAA GCA TGG TAG ATG TTG ATT AAT CTC TTT TCA TTT TAA TGT ACA TTA AAA ATG TGG CGA ATT CGA GCT CGT TTA AAC [3]
BAM36	GCG CTG AAA GCA TTA CAA GTG GG
BAM37	GGG GAT CCG TCG ACC TGC AGC GTA CGA GCT ATC CTC ATC CTC GGT C
BAM38	GTT TAA ACG AGC TCG AAT TCA TCG ATG GTA GCT TAA AGT CAC ACC G
BAM39	GCA AGA GGA GAT GAG ACT CC
BAM31	CCG TAC TCC TAC ACG GGA G
BAM32	GGG GAT CCG TCG ACC TGC AGC GTA CGA ATC TTC ATC TTC AAT CGG
BAM33	GTT TAA ACG AGC TCG AAT TCA TCG ATC CGA ACT ATT TAA CAT ATC C
BAM34	GGA AGT CTG ATA TTA CAA CC

[1] *S. cerevisiae LEU2* sequence underlined. [2] *kanMX4* sequence underlined. [3] *kanMX6* sequence underlined. [4] *Xho*I site underlined. [5] *Xba*I site underlined.